CHAPTER IV

RESULTS

1. Isolation of fungi

Aureobasidium spp. were successfully isolated from several habitats in various locations in Thailand (Table 5). Isolates were obtained from diverse areas: Bangkok, Loburi, Nakornratchasrima, and Songkhla provinces which are in the central, northeastern and southern Thailand (Figure 12). Habitats included plant leaves and painted buildings and bathroom cement walls. It is important to note that *Aureobasidium* was not always recovered. No isolates were recovered from a range of leaves including *Artocarpus heterophyllus* Lam.(Jack fruit), *Annona squamosa* Linn.(Custard apple), *Averrhoa bilimbi* Linn. (Cucumber tree), *Bambusa multiplex* Lour., *Bauhinia tomentosa* Linn., *Bougainvillea spectabilis* Linn., *Cassia fistula* Linn.(Golden shower), *Desmos chinensis* Lour., *Eugenia uniflora* Linn.(Cayenne cherry), *Hibiscus rosa-sinensis* Linn. (Hibiscus), *Phyllantus acidus* Linn. Skeels. (Star gooseberry), *Polyalthia longifolia*, *Manilkara zopota* Linn.(Nasebery), *Psidium guajava* Linn. (Guava), *Sandoricum koetjape* (Burm.f.) Merr., and *Thuja orientalis*. In my isolations no cultures were recovered from Pitsanulok province.

Other fungal genera routinely recovered included: *Aspergillus*, *Cladosporium*, *Penicillium*, *Rhizopus,* and *Trichoderma.*

Nine (9) isolates of *Aureobasidium* spp. were recovered using MEA half-strength agar while other six (6) isolates were recovered using CMA half-strength.

Figure 12 Sampling sites in Thailand where *Aureobasidium* spp. were found.

Table 5 *Aureobasidium* spp. isolated from habitats and locations in Thailand

Isolates	Habitats	Locations	Culture media
BK1	Bathroom cement wall	Bangkok	CMA
BK2	Leaf of mango (*Mangifera indica* Linn.)	Bangkok	CMA
BK3	Leaf of tamarind (*Tamarindus indica* Linn.)	Bangkok	MEA
BK4	Building latex painted surface	Bangkok	MEA
BK5	Flower of *Ochna kirkii* Oliv.	Bangkok	MEA
BK6	Bathroom cement wall	Bangkok	MEA
BK7	Leaf of *Ochna kirkii* Oliv.	Bangkok	MEA
NRM1	Leaf of rain tree (*Albizia saman* (Jacg.) F. Muell.)	Nakornratchasrima	CMA
NRM2	Leaf of asoka (*Saraca indica* Linn.)	Nakornratchasrima	CMA

Table 5 (cont.) *Aureobasidium* spp. isolated from habitats and locations in Thailand

Isolates	Habitats	Locations	Media used
LB1	Leaf of tamarind (*Tamarindus indica* Linn.)	Loburi	MEA
LB2	Leaf of tamarind (*Tamarindus indica* Linn.)	Loburi	CMA
LB3	Leaf of asoka (*Saraca indica* Linn.)	Loburi	MEA
SK1	Leaf of *Syzygium malaccense Linn.*	Songkhla	MEA
SK2	Leaf of asoka (*Saraca indica* Linn.)	Songkhla	CMA
SK3	Leaf of tamarind (*Tamarindus indica* Linn.)	Songkhla	MEA

2. Fungal identification

2.1 Morphological examination

2.1.1 Colony characteristics

The recovered colonies of all isolates were examined after growth on solid culture medium (MEA) for 7 days (Figures 13–16). The isolates grew rapidly. Colonies were smooth, slimy and creamy, though some colonies became black with time. Indeed most colonies were black. However, colonies of isolates NRM2 and LB3 were pink while those of isolates LB2 and SK3 were red and yellow, respectively. The colony sizes ranged between 2.86 and 4.75 cm. on the MEA after 7 days.

2.1.2 Microscopic observation

Examination of the cell morphology of the isolates by bright-field light microscopy showed the classic *A. pullulans* polymorphology with blastospores, chlamydospores, conidia and hyphae. Some isolates had swollen cells and blastoconidia. Hyphae were septate, thin-walled, and hyaline, but became thicker and black in late culture except for the color variants, conidia were hyaline, smooth, ellipsoidal, and variable in size and shape. Secondary conidia and endoconidia were observed. Large swollen cells and dark thick-wall chlamydospores were also revealed. The size of conidia, blastospore, and chlamydospores ranged from 2x5 μm to 8x10 μm. The morphology of the cells grown in solid and liquid culture media is illustrated in Figures 17-31.

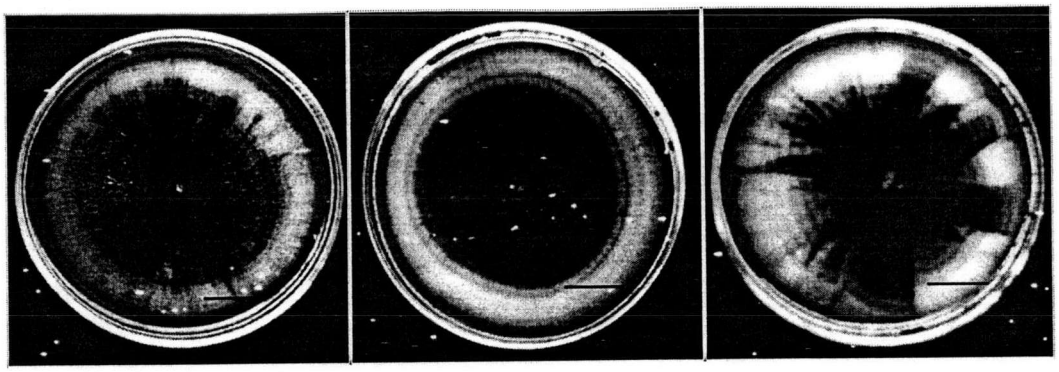

BK1 BK2 BK3

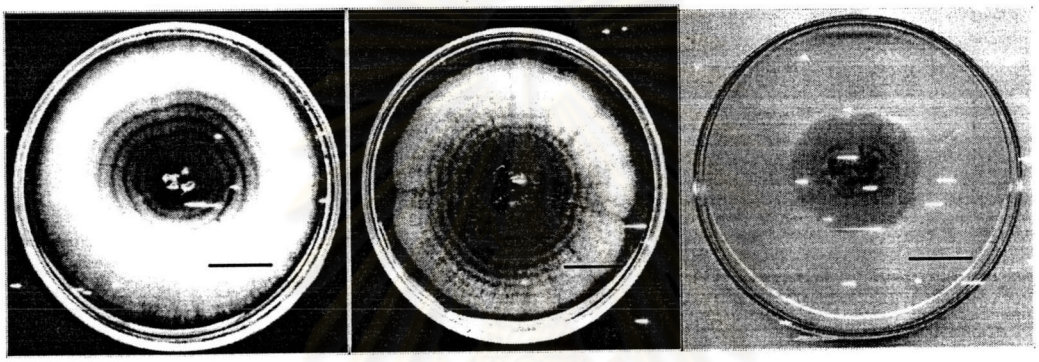

BK4 BK5 BK6

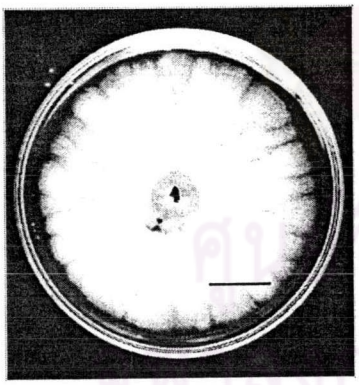

BK7

Figure 13 Colony characteristic of *Aureobasidium* isolates from Bangkok area

—— = 2.5 cm.

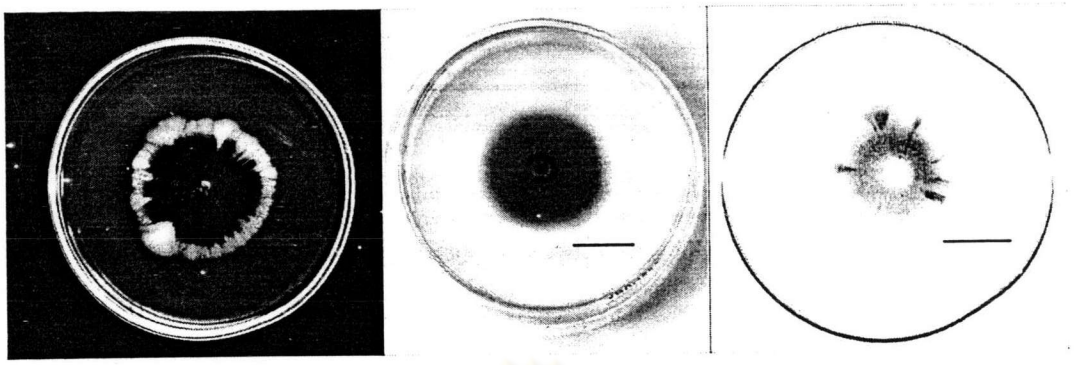

LB1 LB2 LB3

Figure 14 Colony characteristic of *Aureobasidium* isolates from Loburi area

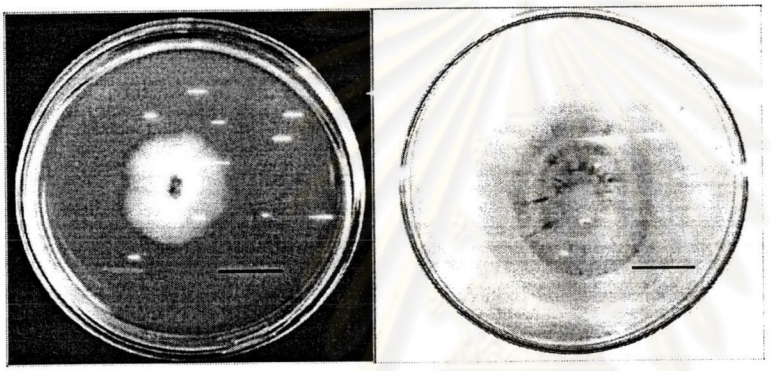

NRM1 NRM2

Figure 15 Colony characterisctic of *Aureobasidium* isolates from Nakornratchasrima area

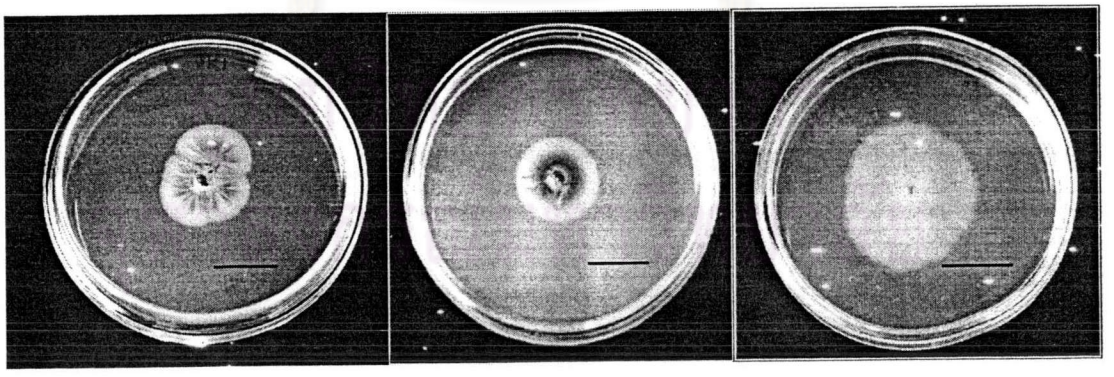

SK1 SK2 SK3

Figure 16 Colony characteristic of *Aureobasidium* isolates from Songkhla area

—— = 2.5 cm.

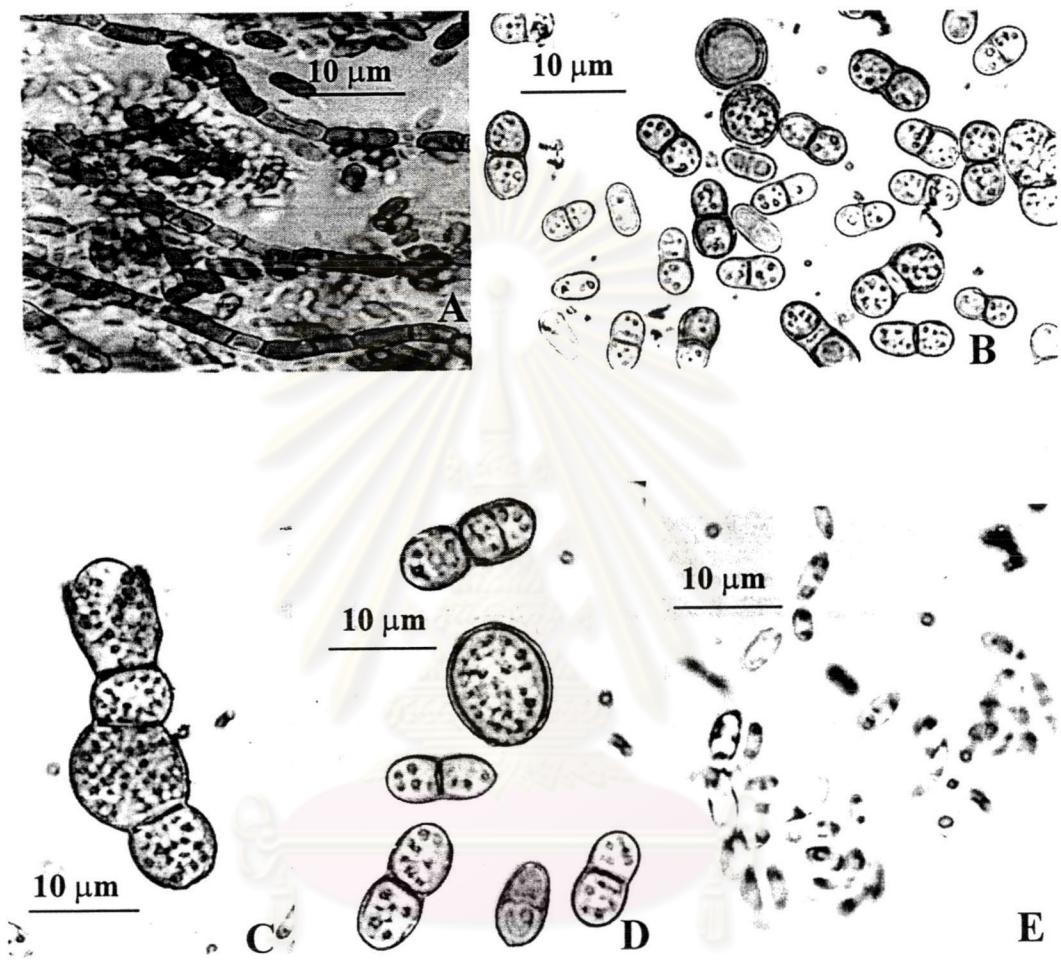

Figure 17 Morphology of isolate BK1. (A) hyphae, (B) dark swollen cells, arthroconidia, and chlamydospores, (C) dark chlamydospore, (D) dark swollen cell and arthroconidia, (E) conidia

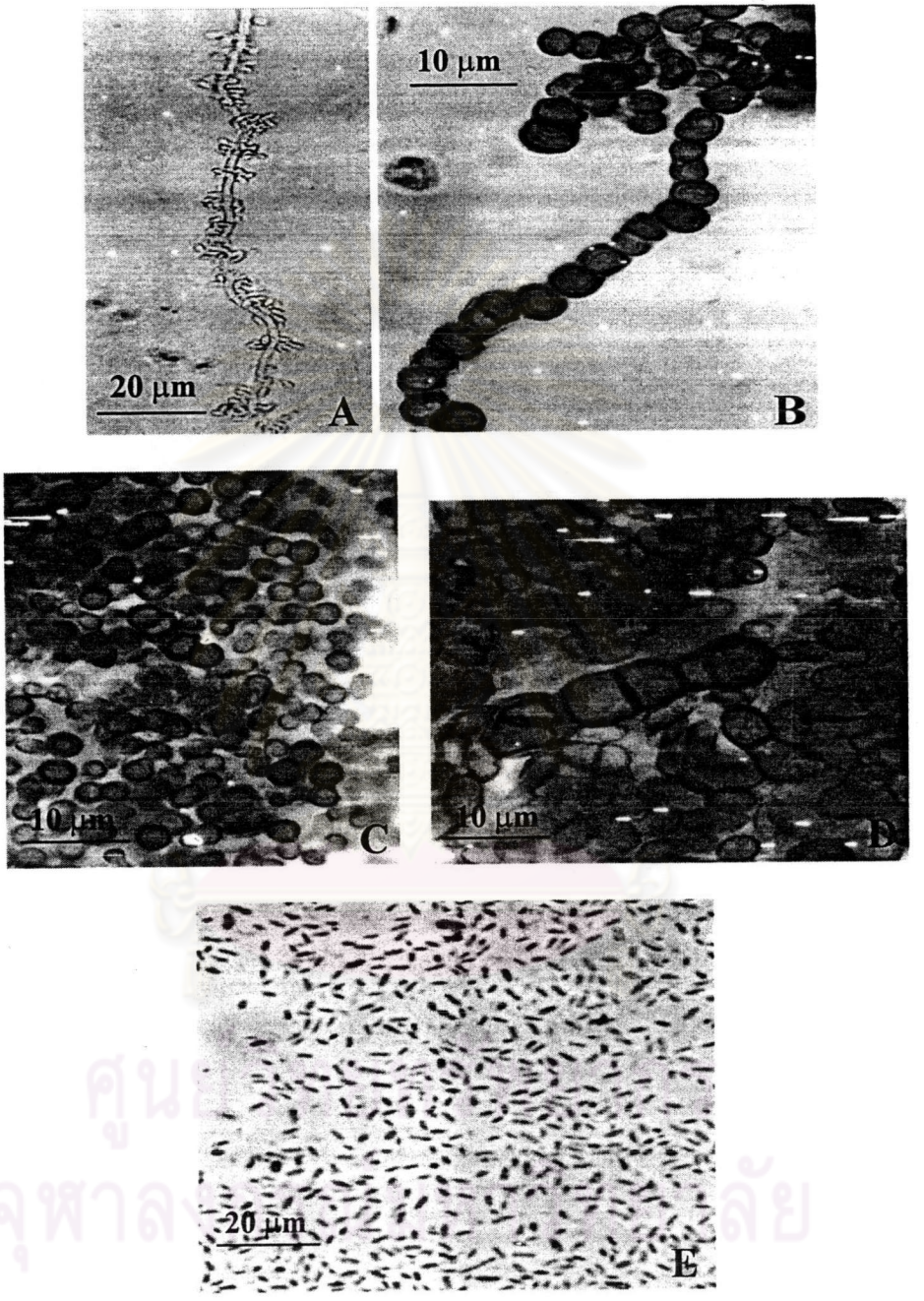

Figure 18 Morphology of isolate BK2. (A) hyaline hypha, (B) dark hyphae, (C) dark chlamydospores and arthroconidia, (D) dark chlamydospores and arthroconidia, (E) conidia

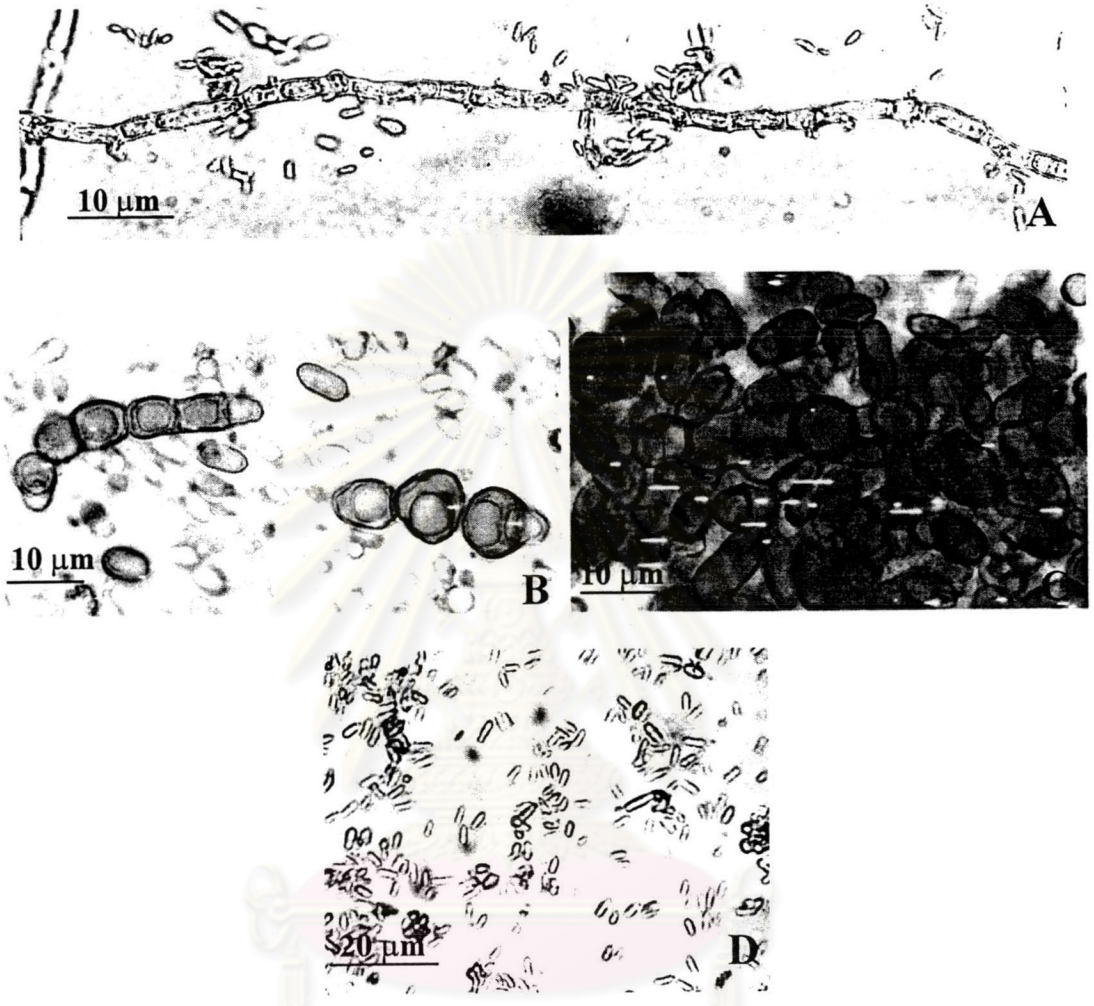

Figure 19 Morphology of isolate BK3. (A) hyaline hypha, (B) dark arthroconidia, (C) dark chlamydospores and arthroconidia, (D) conidia.

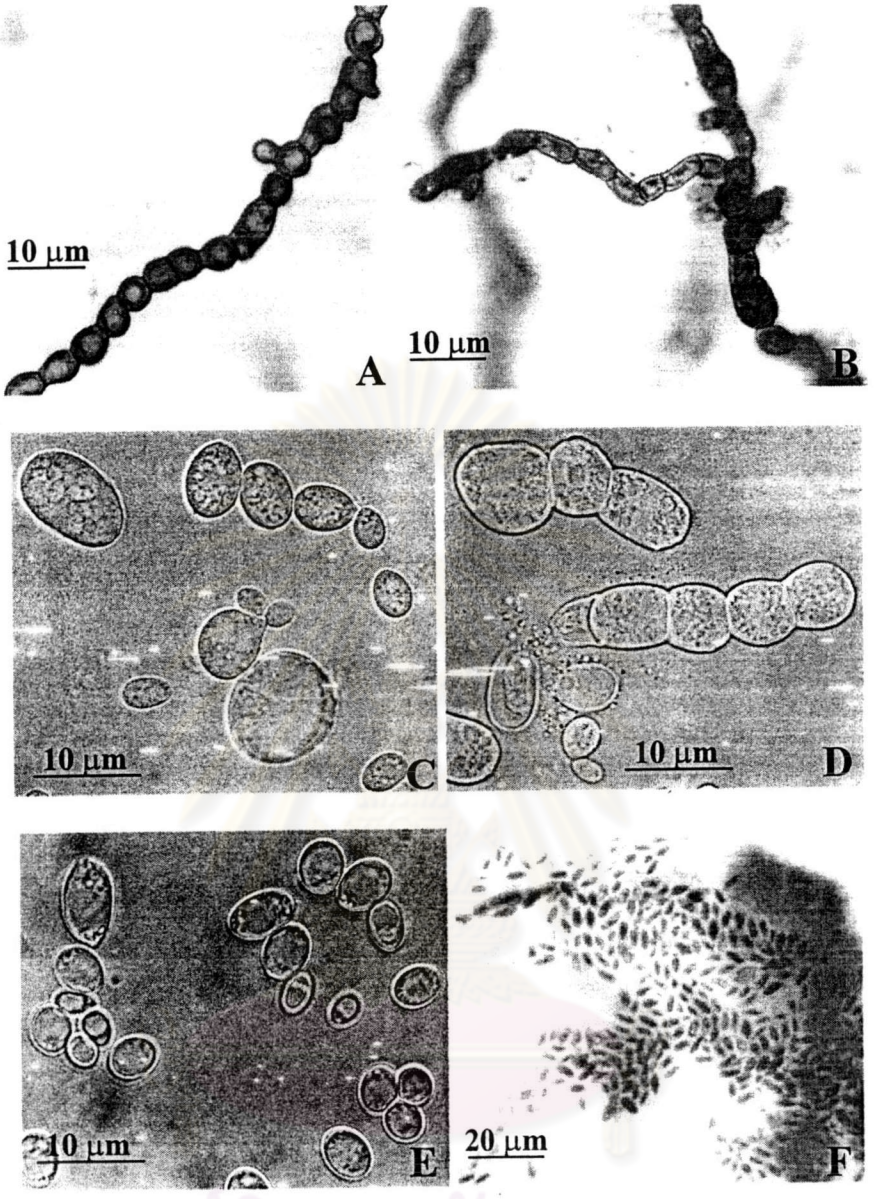

Figure 20 Morphology of isolate BK4. (A) dark hypha, (B) hypha, (C) swollen cell and blastospores, (D) chlamydospores, (E) blastospores, (F) conidia

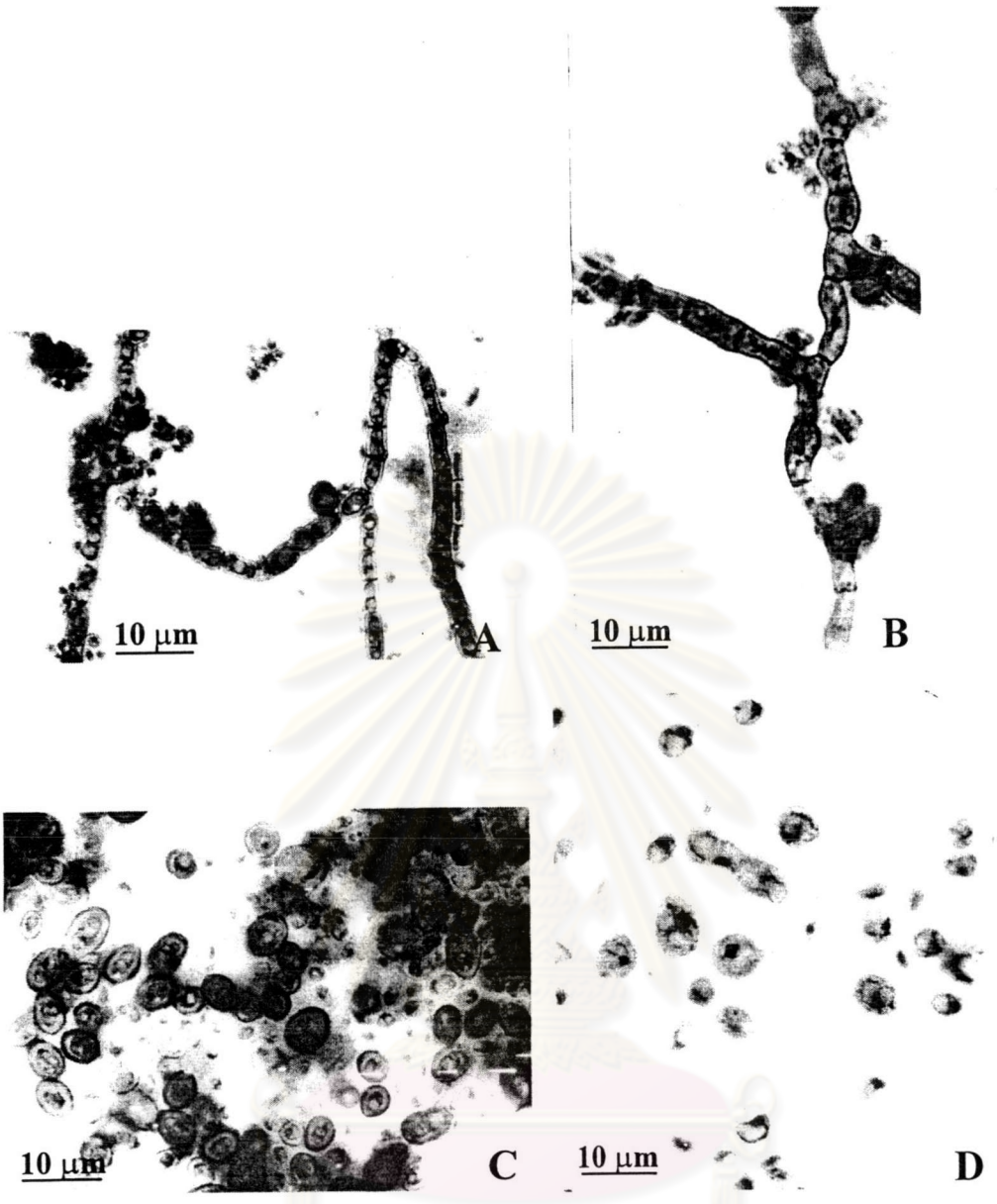

Figure 21 Morphology of isolate BK5. (A) hyphae, (B) hypha with conidia, (C) blastospores, (D) conidia

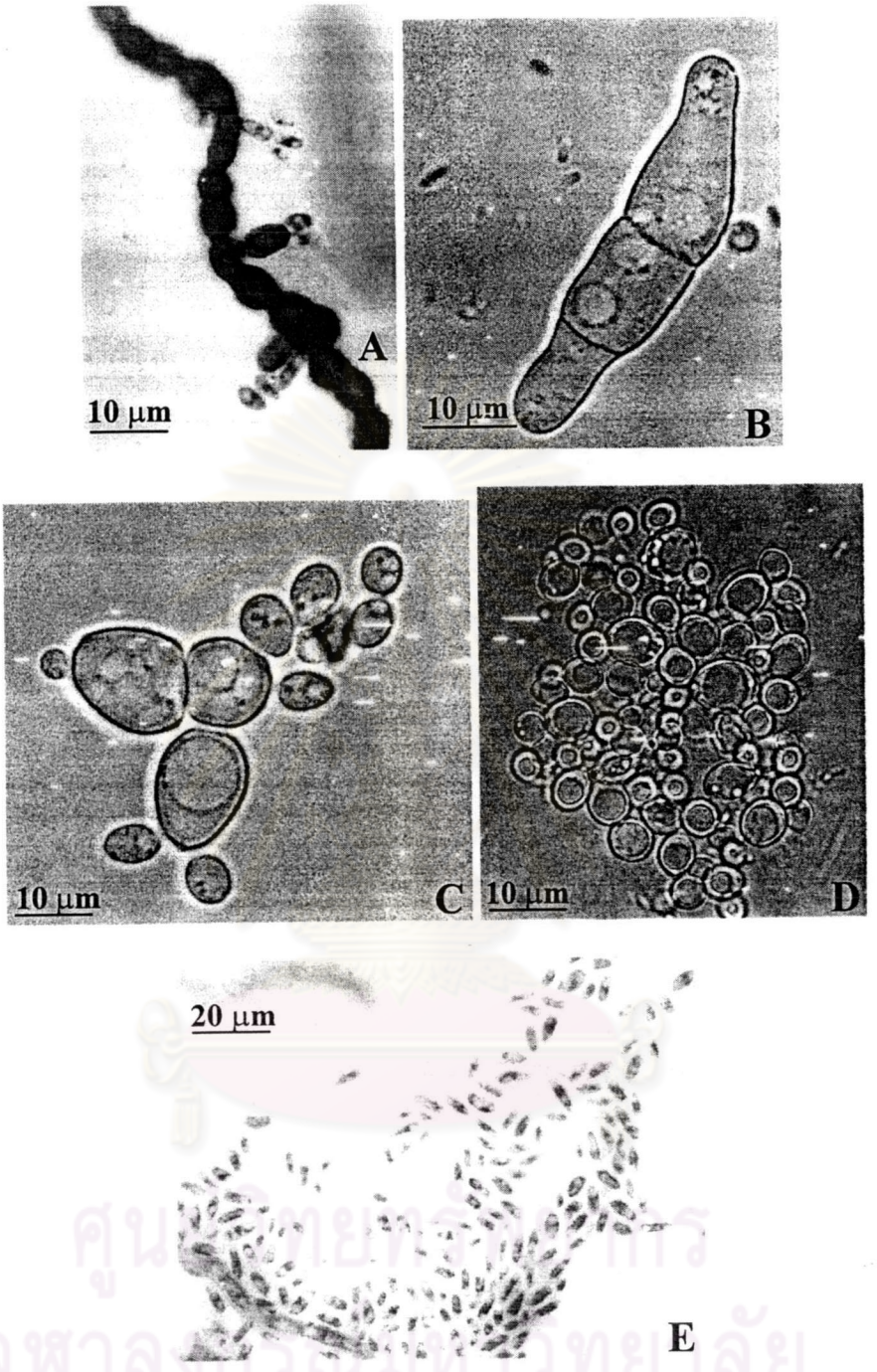

Figure 22 Morphology of isolate BK6. (A) hypha and conidial apparatus, (B) chlamydospore, (C) blastospores and budding, (D) blastospores, (E) conidia

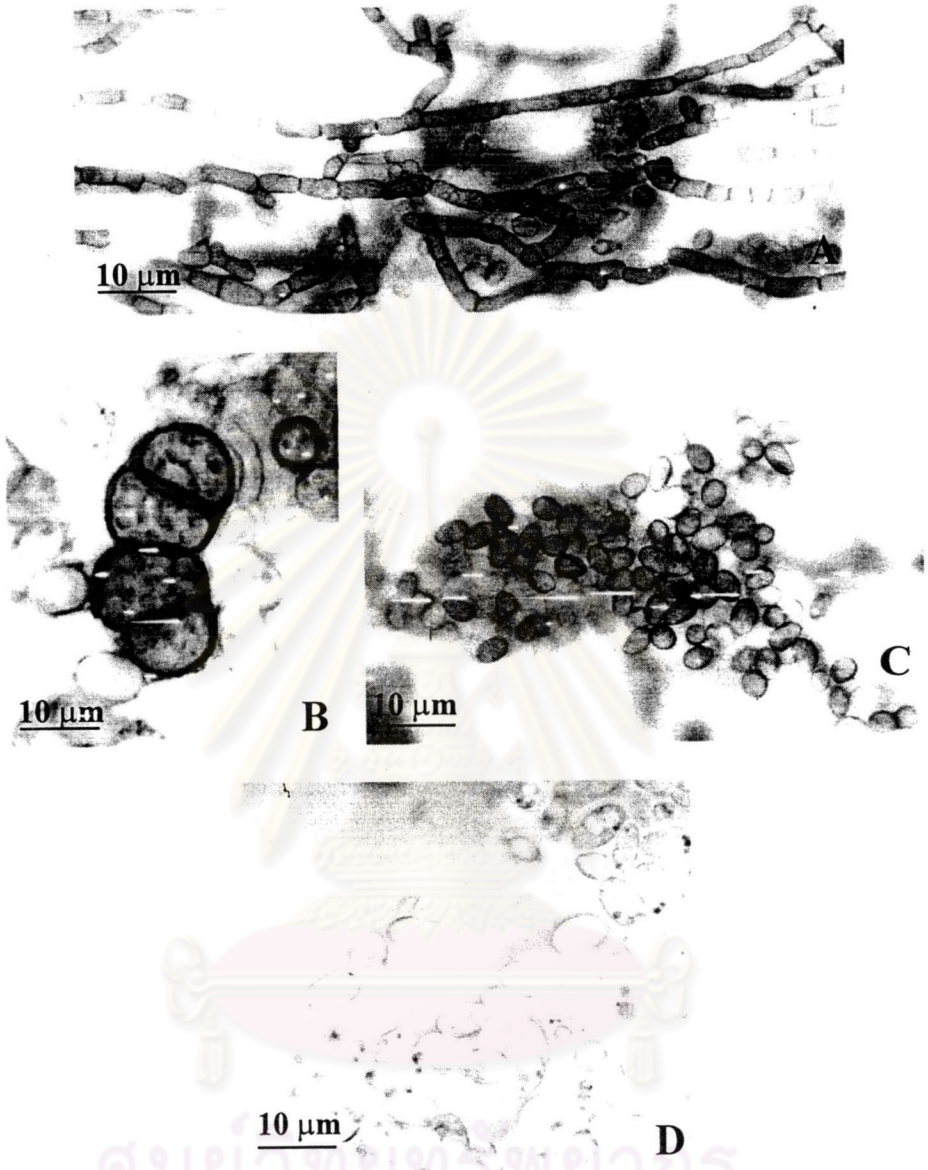

Figure 23 Morphology of isolate BK7. (A) hyphae, (B) chlamydospore, (C) dark arthroconidia, (D) blastospores

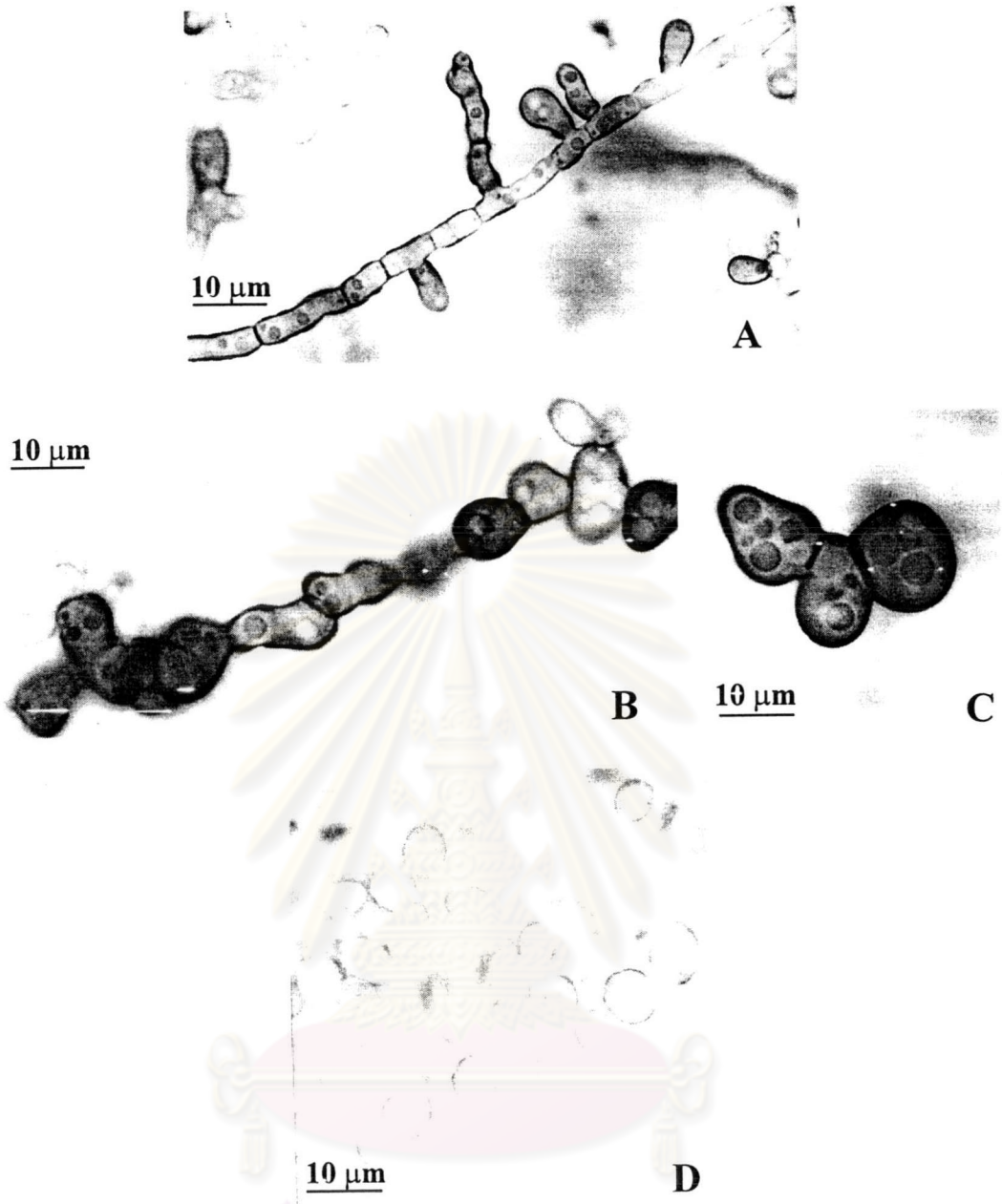

Figure 24 Morphology of isolate LB1. (A) hypha, (B) hypha with conidia, (C) dark chlamydospore, (D) blastospores

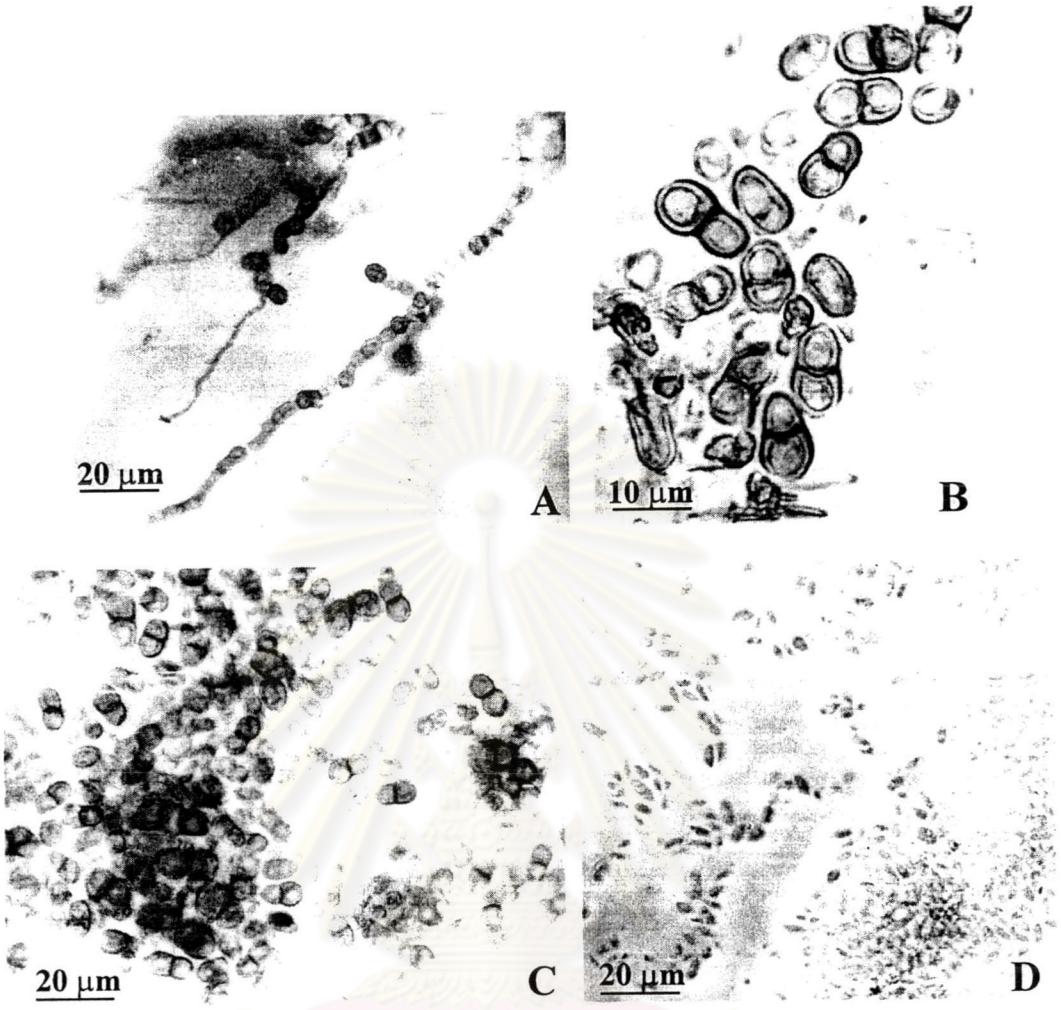

Figure 25 Morphology of isolate LB2. (A) hypha, (B) dark arthroconidia, (C) group of dark arthroconidia, (D) conidia

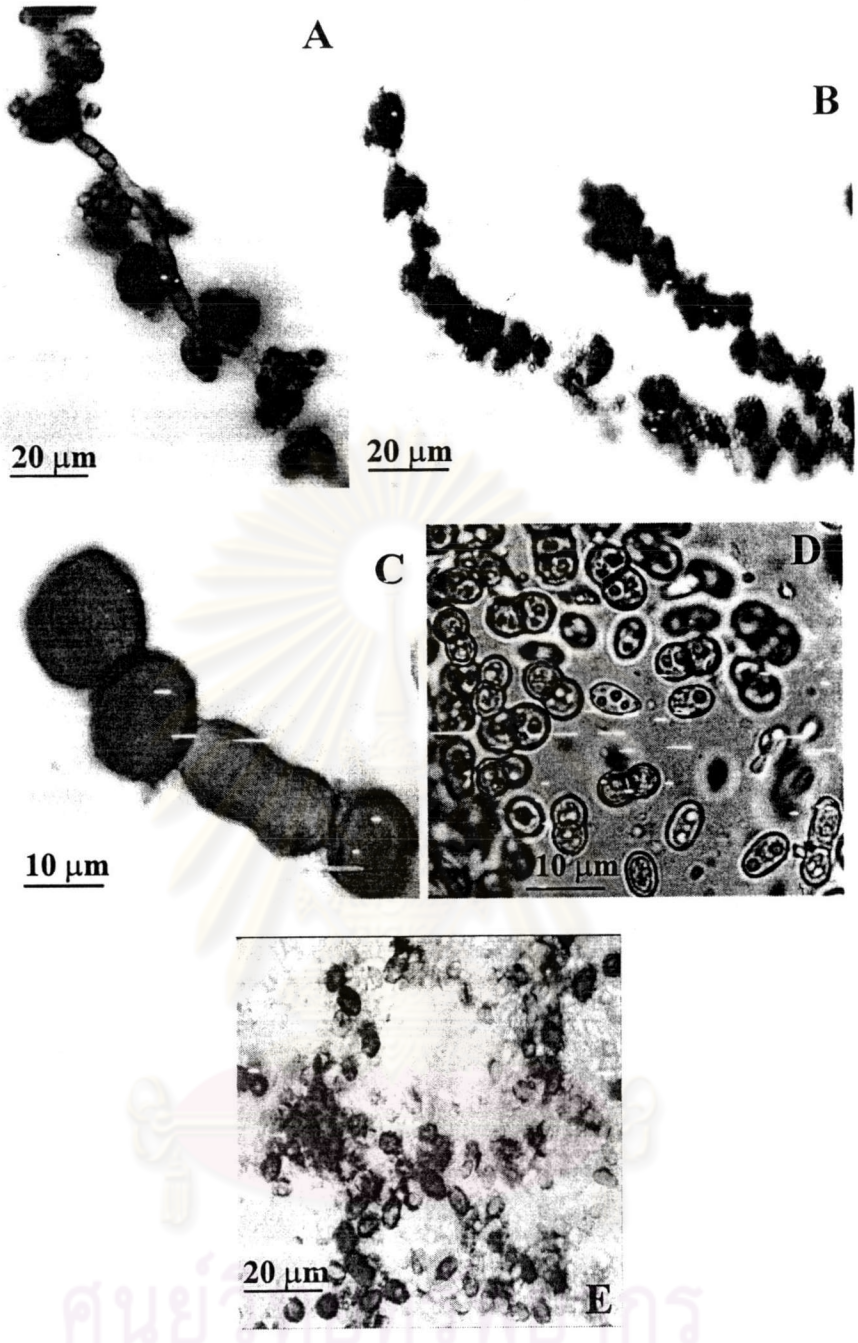

Figure 26 Morphology of isolate LB3. (A) hypha with conidia, (B) hyphae with conidia, (C) chlamydospore, (D) dark chlamydospores and blastospores, (E) dark arthroconidia and conidia

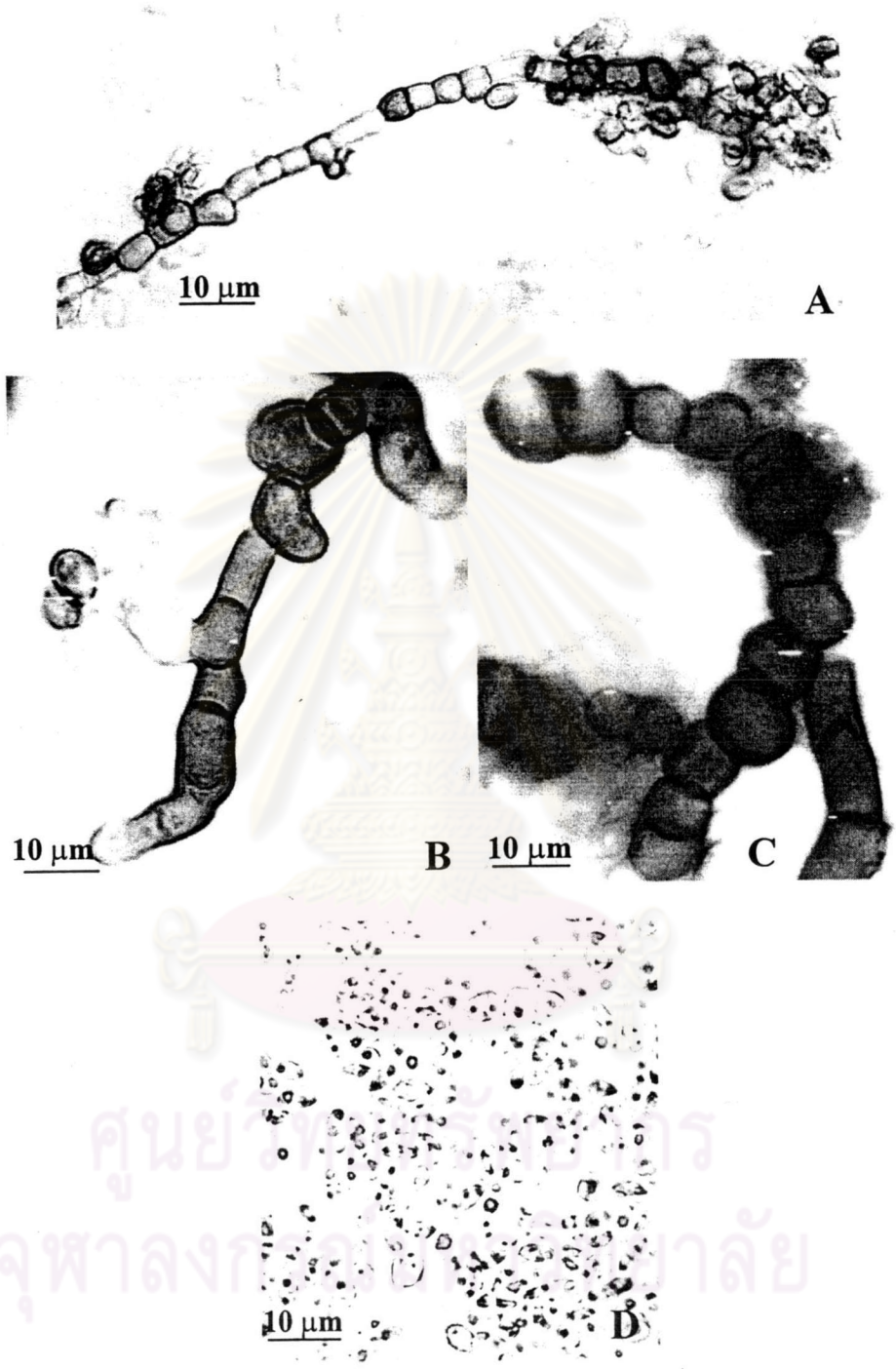

Figure 27 Morphology of isolate NRM1. (A) hypha, (B) dark hypha with conidia, (C) dark hyphae, (D) conidia

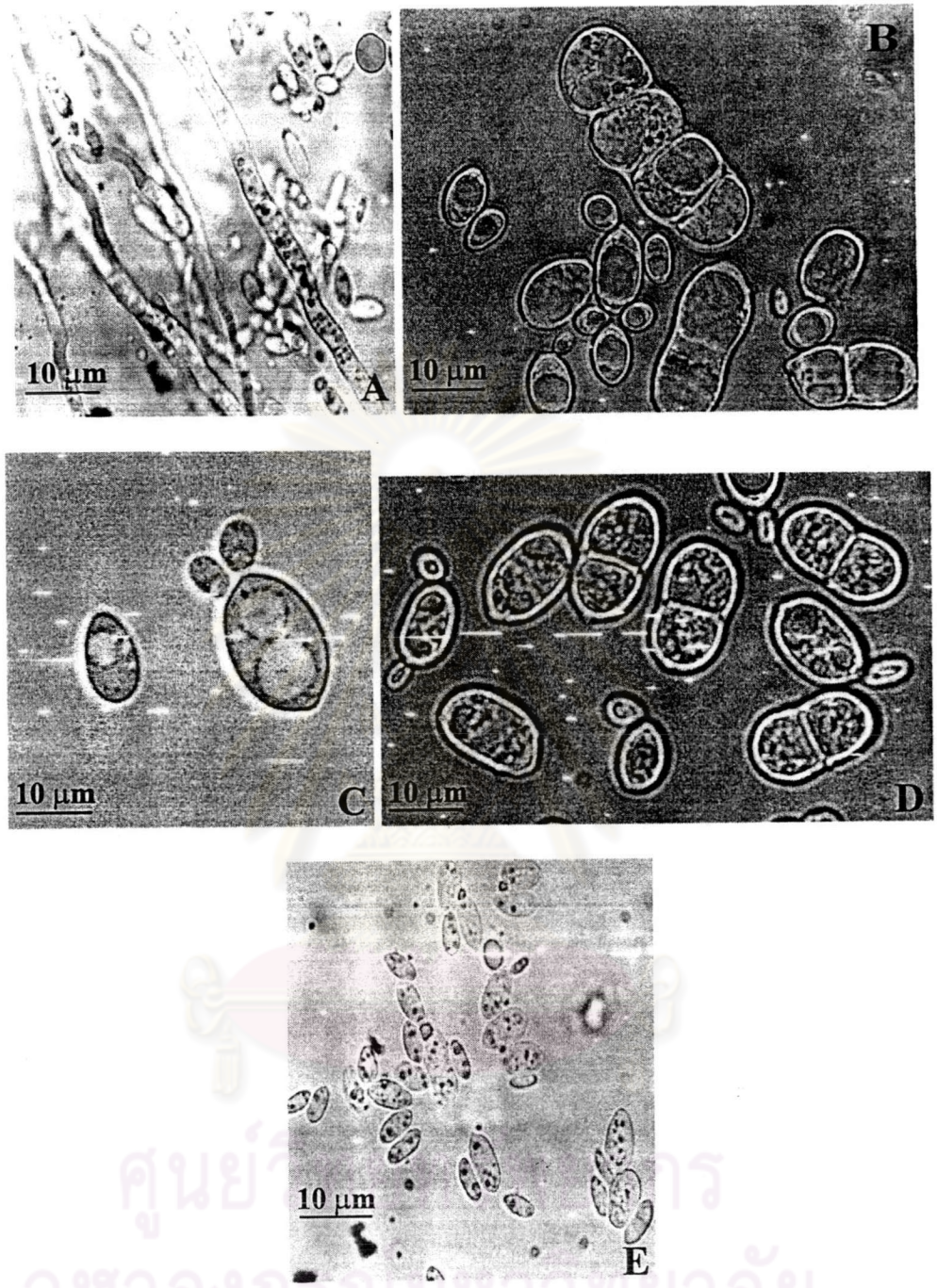

Figure 23 Morphology of isolate NRM2. (A) hypha, (B) hlamydospores and blastospores, (C) blastospores with budding, (D) arthroconidia and blastospores, (E) conidia

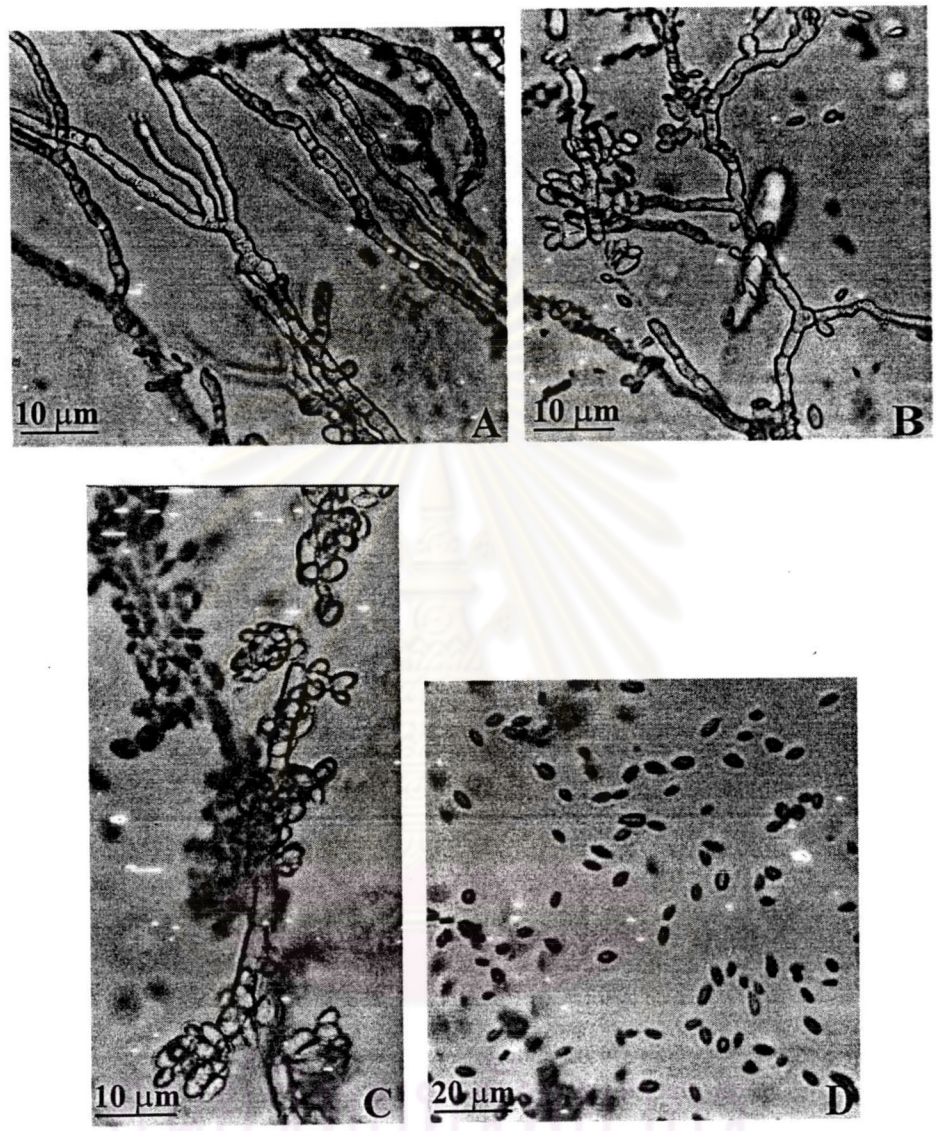

Figure 29 Morphology of isolate SK1. (A) hyphae, (B) hyphae with conidia, (C) hyphae with several groups of conidia, (D) conidia

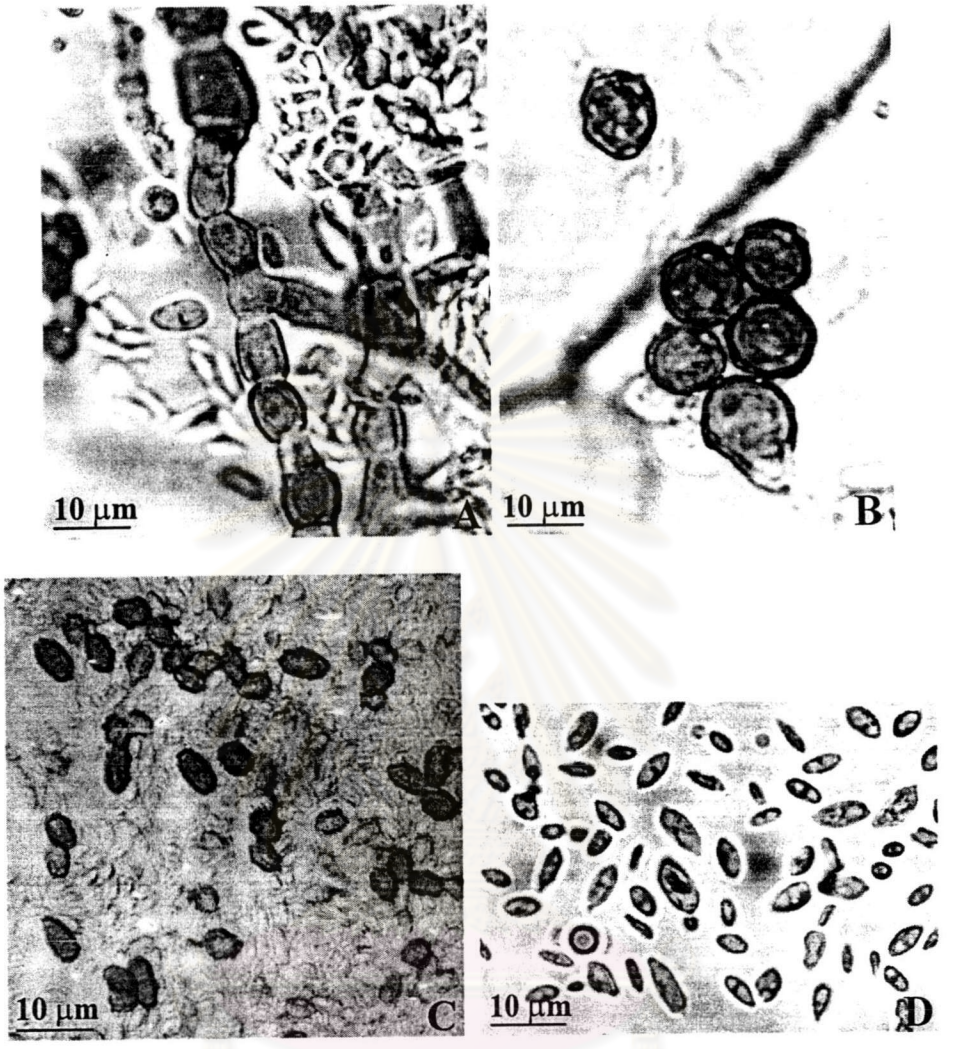

Figure 30 Morphology of isolate SK2. (A) hyphae, (B) dark chlamydospores, (C) dark arthroconidia, (D) conidia

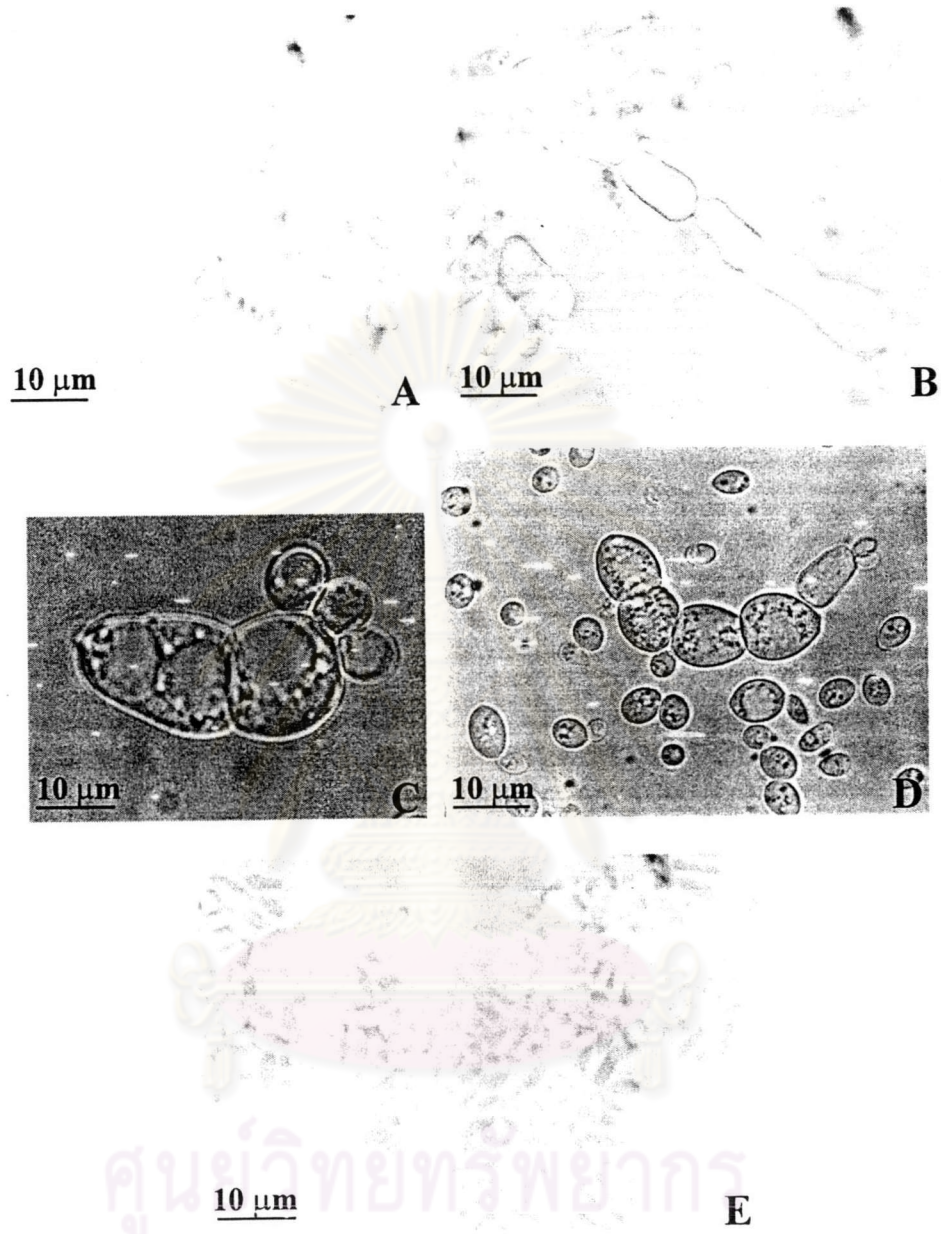

Figure 31 Morphology of isolate SK3. (A) hypha, (B) hypha with conidia, (C) blastospore with budding, (D) chlamydospores and blastospores, (E) conidia

2.2 Nuclear Ribosomal DNA Internal Transcribed Spacer (ITS) sequencing.

Five isolates of *Aureobasidium* spp. (BK4, BK6, LB3, NRM2, and SK3) were taxonomically assessed by ITS sequencing. The PCR products of the ITS region are ranged between 650 to 850 bp, the appropriate size of the ITS region (Figure 32). Sequences of isolates BK4, BK6, LB3, NRM2, and SK3 were identical as assessed using the ClustalW program, and also identical to other *A. pullulans* in GenBank (using BLAST program), including: AF121284 (ATCC 42457), AY139395 (CBS 110373), AY 139393 (CBS 110376), AY139392 (CBS 110375), AJ244236 (CBS 101160), AY139391 (CBS 110377), AJ244269 (VKPM F-371), AJ276062 (MZ 58) and AJ276061 (MZ65) (Figure 33). The sequence for SK3 differed slightly from the other four by a single T to A transversion in the ITS1 (Figure 35) and a single deletion (T) in the ITS 2 (Figure 36). Strain SK3 sequence was more similar to those of isolates BK4, BK6, NRM2, and LB3 than to sequences in GenBank, namely the following accession numbers: AY225163, AY225164, AY225165, AY225166, AY225167, respectively for the isolates BK4, BK6, NRM2, SK3, and LB3. A phylogenetic tree of these *Aureobasidium* isolates was constructed using the PAUP program based on these ITS sequences (Figure 34). A black yeast *Pringsheimia* sp. was used as an out-group fungus. The ITS sequence of isolate SK3 slightly differed from those of the other four. The constructed phylogenetic tree was able to confirm that they still belongs to the same cluster with other isolates and *A. pullulans* strains in GenBank.

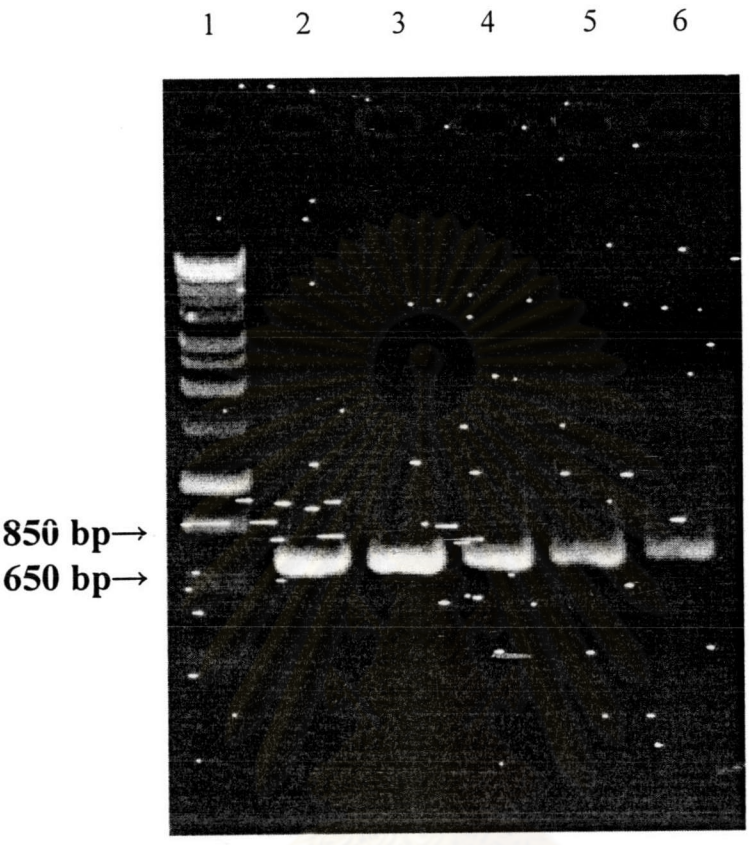

Figure 32 PCR products of ITS region for all five Thai isolates on agarose gel electrophoresis

Lane 1: 1 kb DNA loading marker

Lane 2: PCR product of ITS region from isolate BK4

Lane 3: PCR product of ITS region from isolate BK6

Lane 4: PCR product of ITS region from isolate LB3

Lane 5: PCR product of ITS region from isolate SK3

Lane 6: PCR product of ITS region from isolate NRM2

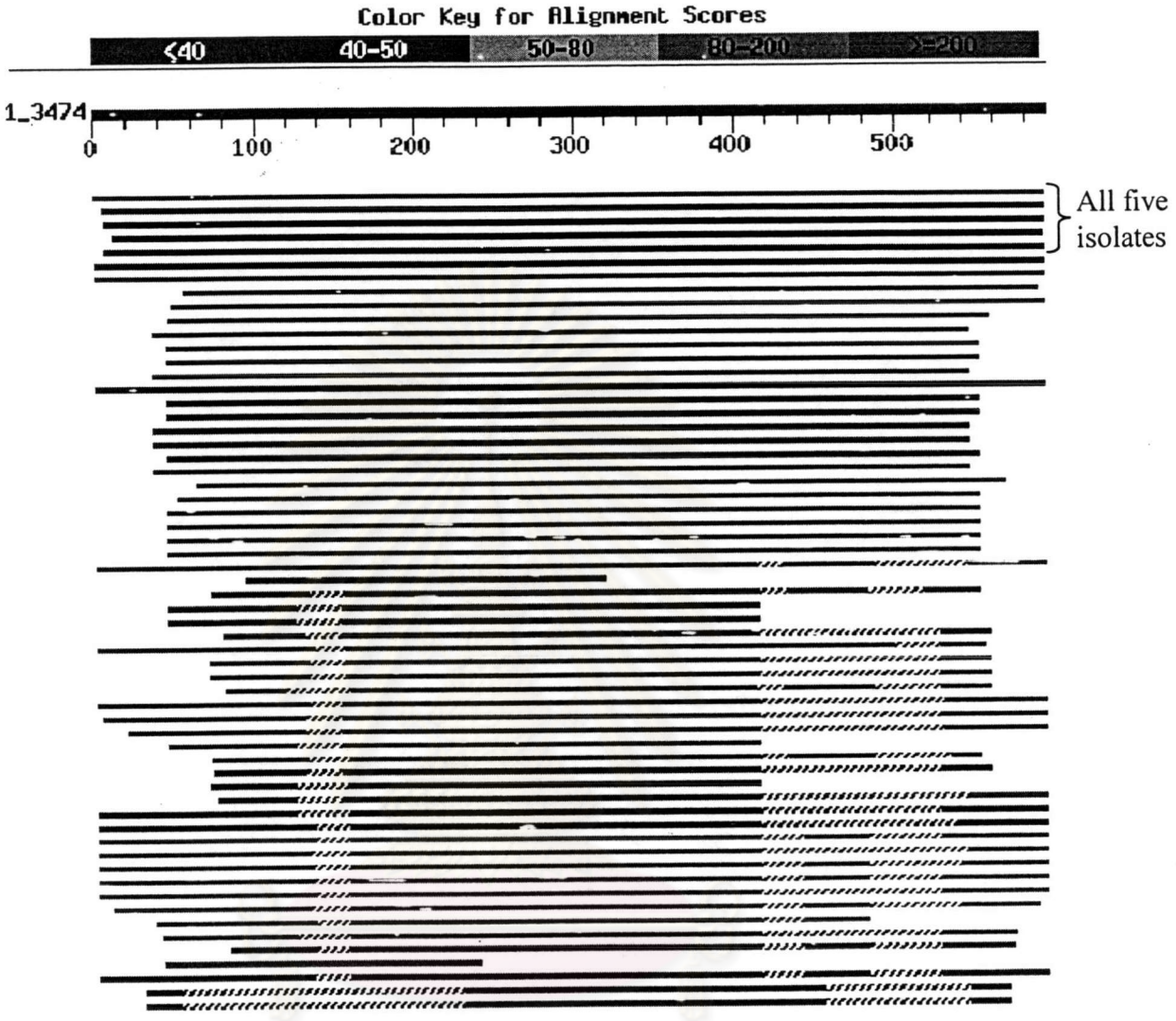

Figure 33 BLAST results of Thai *Aureobasidium* isolates compared with other *A. pullulans* in GenBank

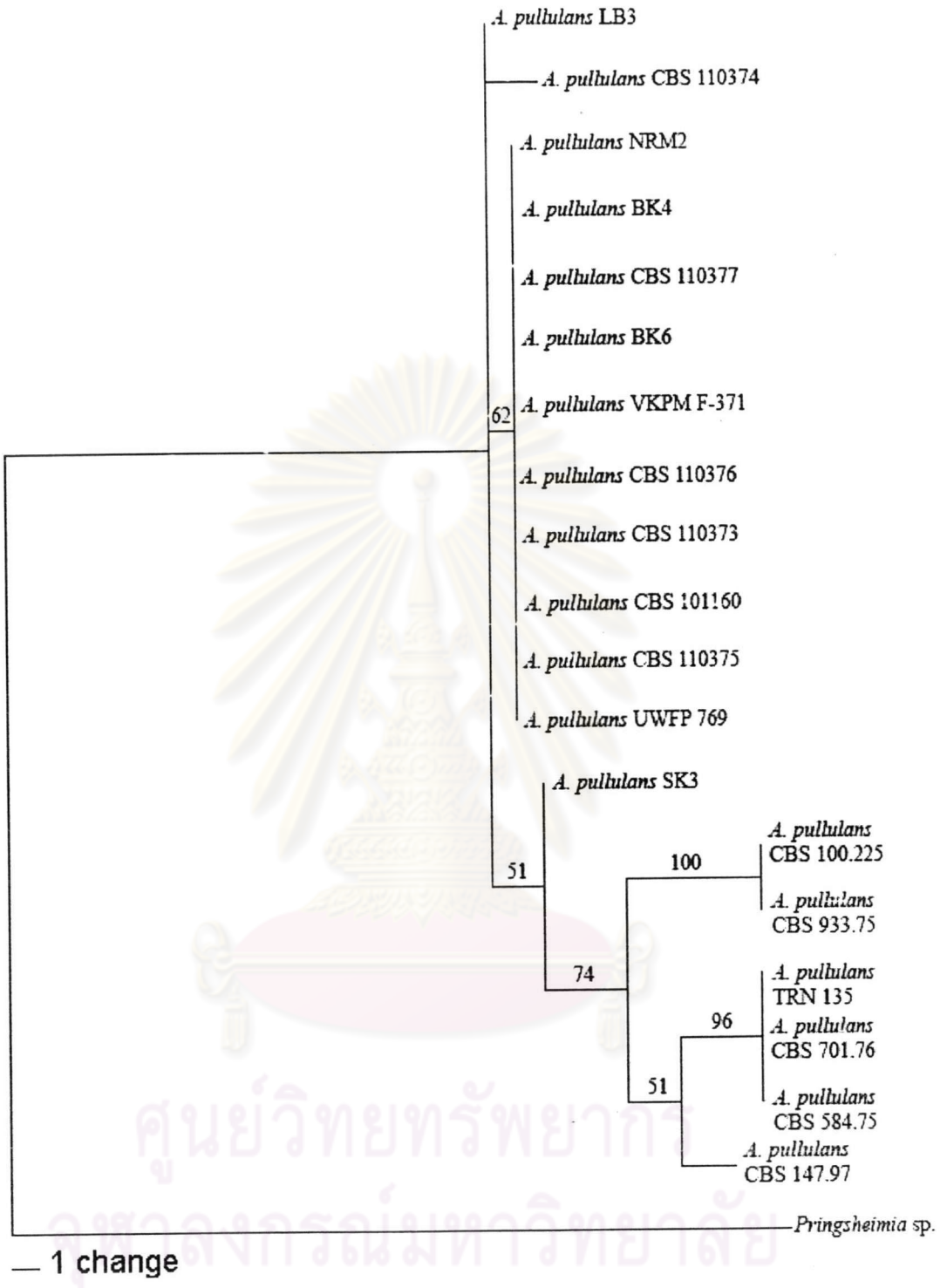

Figure 34 Neighbor-joining tree of *A. pullulans* isolates based on ITS sequences

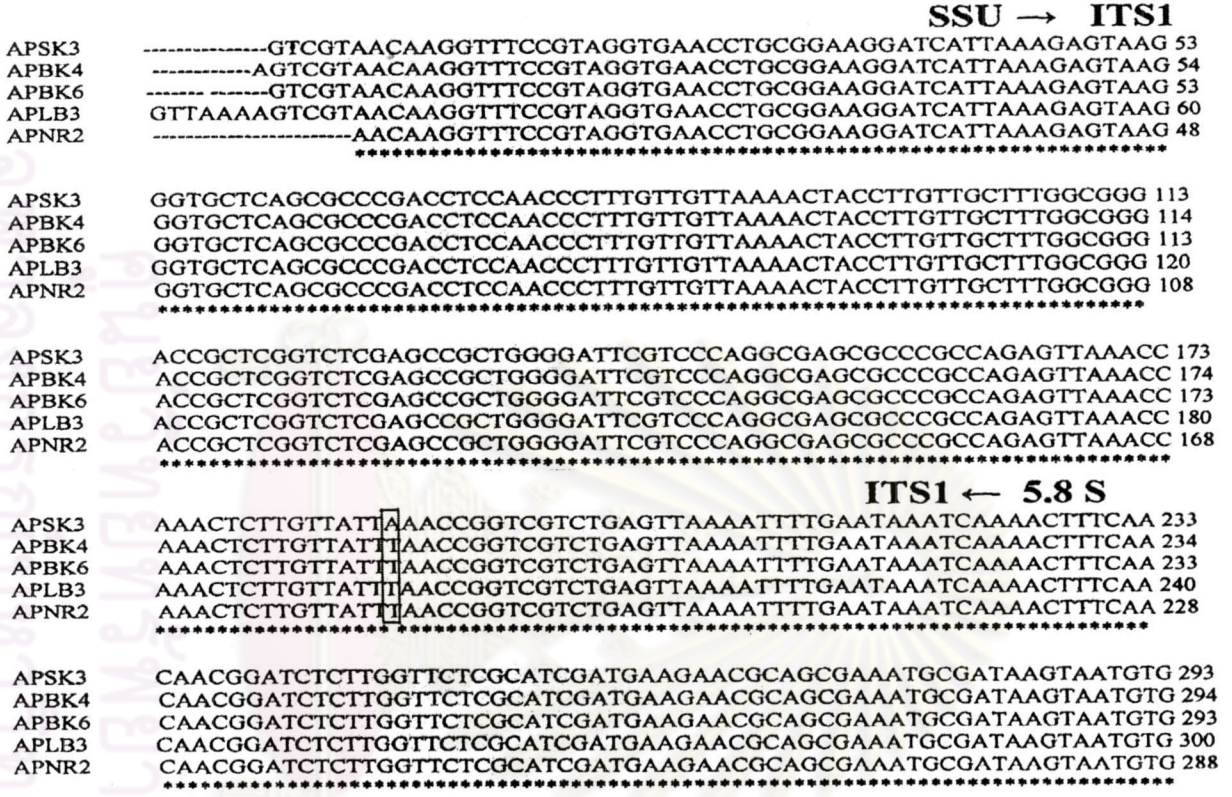

Figure 35 Clustal W analysis of ITS1 sequences of *Aureobasidium* isolates (APSK3= *Aureobasidium* SK3, APBK4= *Aureobasidium* BK4, APBK6= *Aureobasidium* BK6, APLB3= *Aureobasidium* LB3, and APNR2= *Aureobasidium* NRM2)

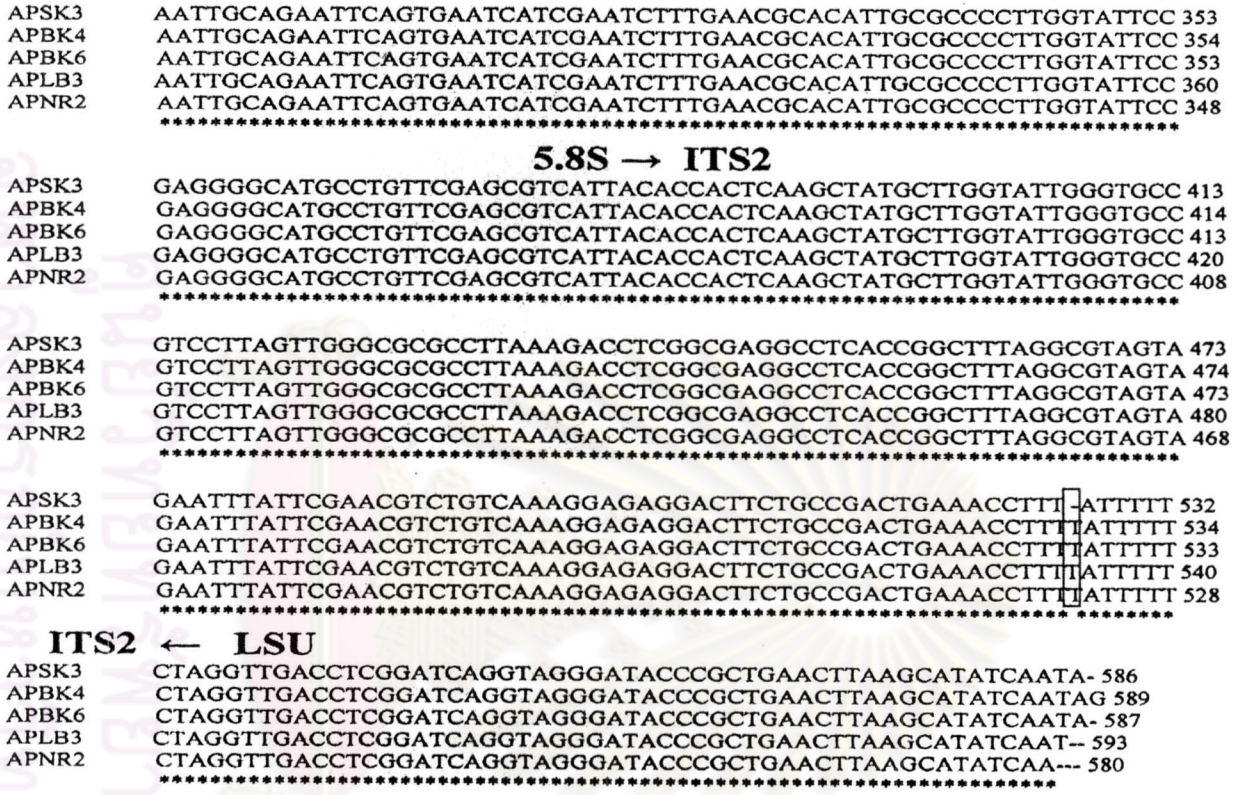

Figure 36 Clustal W analysis of ITS 2 sequences of *Aureobasidium* isolates (APSK3= *Aureobasidium* SK3, APBK4= *Aureobasidium* BK4, APBK6= *Aureobasidium* BK6, APLB3= *Aureobasidium* LB3, and APNR2= *Aureobasidium* NRM2)

2.3 Nutritional physiology tests

The carbon and nitrogen assimilation patterns of the isolates correlated with the assimilation patterns of the control strains (Tables 6 and 7). A diverse range of carbon sources was utilized including cellobiose, dulcitol, fructose, galactose, glucose, glycerol, methyl-α-D-glucoside, raffinose, sucrose, xylitol, and xylose. Cellulose, chitin, p-coumaric acid, sodium succinate, and sodium salicylate were not assimilated. Intra-specific variation of *Aureobasidium* isolates and standard strains was found in the assimilation of dulcitol, glucosamine, glycerol, rhamnose, and sodium citrate (Table 6). Nitrogen sources that were utilized included L-arginine, creatinine HCl, L-isoleucine, L-lysine, L-serine, sodium nitrate, sodium nitrite, and L-tryptophane but not creatine monohydrate, and L-threonine. Different cell growth in nitrogen assimilation among the isolates and standard strains was observed in L-alanine, L-glutamine, L-glycine, L-proline, and L-phenylalanine (Table 7).

Table 6 Carbon assimilation pattern of *Aureobasidium* isolates from Thailand.

Carbon substrates\ Strains	BK4	BK6	SK3	NRM2	LB3	NRRL Y-2311-1*	NRRL Y-7469*
1. Caffeic acid	-	-	w	-	-	-	-
2. D-cellobiose	+	+	+	+	+	+	+
3. Cellulose powder (1% fibrous)	-	-	-	-	-	-	-
4. Chitin (colloidal)	-	-	-	-	-	-	-
5. p-Coumaric acid	-	-	-	-	-	-	-
6. Dulcitol	+	+	+	+	+	-	+
7. Fructose	+	+	+	+	+	+	+
8. D-Galactose	+	+	+	+	+	+	+
9. D-(+)-glucosamine	w	w	-	-	-	+	-
10. D-glucose	+	+	+	+	+	+	+
11. Glycerol	+	+	w	+	+	w	w
12. Lactose	+	+	+	+	+	+	+
13. Maltose	+	+	+	+	+	+	+
14. Mannitol	+	+	+	+	+	+	+
15. α-Methyl-D-glucose	+	+	+	+	+	+	+
16. Myo-inositol	+	+	+	+	+	+	+
17. Quinic acid	+	+	+	+	+	+	+
18. Raffinose	+	+	+	+	+	+	+
19. Rhamnose	+	+	-	+	+	+	+
20. Ribose	+	+	+	+	+	+	+
21. Sodium acetate	-	-	-	-	-	-	w
22 Sodium citrate	-	-	-	-	+	+	+
23. Sodium salicylate	-	-	-	-	-	-	-
24. Sodium succinate	-	-	-	-	-	-	-
25. D-sorbitol	+	+	+	+	+	+	+
26. Salicin	+	+	+	+	+	+	+
27. Starch (soluble)	+	+	+	+	+	+	+
28. Sucrose	+	+	+	+	+	+	+
29. Trehalose	+	+	+	+	+	+	+
30. D-Xylitol	+	+	+	+	+	+	+
31. D-Xylose	+	+	+	+	+	+	+

* Standard strains, *A. pullulans* NRRL Y-2311-1 and *A. pullulans* NRRL Y-7469

+ = assimilation, - = non assimilation, w = weak assimilation

Table 7 Nitrogen assimilation pattern of *Aureobasidium* isolates from Thailand.

Nitrogen substrates\Strains	BK4	BK6	SK3	NRM2	LB3	NRRL Y-2311-1*	NRRL Y-7469*
1. L-alanine	w	+	+	-	+	+	+
2. L-arginine	+	+	+	+	+	+	+
3. L-asparagine	-	-	-	+	-	+	+
4. L-aspartic acid	+	w	+	+	+	+	+
5. Creatine monohydrate	-	-	-	-	-	-	-
6. Creatinine	+	+	+	+	+	+	+
7. L-glutamic acid	+	+	+	+	+	+	+
8. L-glutamine	+	w	+	-	+	+	+
9. L-glycine	+	+	-	+	+	+	+
10. L-histidine	w	+	+	+	+	+	+
11. L-isoleucine	+	+	+	+	+	+	+
12. L-leucine	+	+	+	-	+	+	+
13. L-lysine	+	+	+	+	+	+	+
14. L-methionine	w	w	+	+	+	+	+
15. L-ornithine	+	w	+	+	+	+	+
16. L-phenylalanine	+	+	+	-	-	+	+
17. L-proline	+	+	+	-	-	+	+
18. L-serine	+	+	+	+	+	+	+
19. Sodium nitrate	+	+	+	+	+	+	+
20. Sodium nitrite	+	+	+	+	+	+	+
21. L-threonine	-	-	-	-	-	-	-
22. L-tryptophane	+	+	+	+	+	+	+
23. L-valine	+	+	+	w	+	+	+

* Standard strains, *A. pullulans* NRRL Y-2311-1 and *A. pullulans* NRRL Y-7469

+ = assimilation, - = non assimilation, w = weak assimilation

3. Exopolysaccharide (EPS) production

A. pullulans were grown in liquid production medium (PM) with initial pH adjusted to 6.5. PM contained glucose (5%) and $(NH_4)_2SO_4$ (0.06%) as carbon and nitrogen sources, respectively. Cultures were cultivated at room temperature (30°C), at 150 rpm for 7 days. The comparative of EPS yields among the isolates are shown Table 8. The comparative EPS yields was obtained from *A. pullulans* BK4 (7.9 $g.l^{-1}$) after 7 days. The factors governing production were optimized for five high-yielding *A. pullulans* isolates (BK4, BK6, LB3, NRM2 and SK3).

3.1 Carbon source and EPS production

Strains were cultivated in production medium containing either glucose or sucrose (5% w/v) with initial pH at 6.5, incubated at room temperature (30°C), 150 rpm for 7 days.

The EPS production profiles of all isolates were similar (Figures 37, 39, 41, 43, and 45). The EPS yields gradually increased from day 1 and reached a maximum yield at day 6-7. The EPS yield from isolates BK4, LB3, and SK3, decreased after 6 days. All isolates gave greater yields on sucrose rather than on glucose. The greatest EPS yield (23.1 $g.l^{-1}$) was produced by isolate BK4 at day 6 with sucrose as carbon source. Highest EPS yields ($g.l^{-1}$) for isolates BK6 (day 7), LB3 (day 6), NRM2 (day 7) and SK3 (day 6) were respectively 17.0, 13.8, 19.6, and 10.4.

3.2 Nitrogen source and EPS production

Nitrogen sources included $(NH_4)_2SO_4$, $NaNO_3$, and peptone. Isolates BK4, BK6 and SK3, with optimal yields on $(NH_4)_2SO_4$ the highest EPS yields ($g.l^{-1}$) being 23.1, 17.0 and 10.4, respectively, and all with sucrose as the carbon source (Figures 38, 40, and 46). Peptone was optimal nitrogen source for isolates NRM2 and LB3

with 25.2 and 15.0 $g.l^{-1}$, respectively, as the highest EPS yield (Figures 42 and 44). None of isolate preferred $NaNO_3$ for EPS production.

Table 8 Comparison of EPS production from *A. pullulans* isolates

Aureobasidium strain	EPS ($g.l^{-1}$)	Production period (day)
BK1	3.7	6
BK2	3.7	7
BK3	4.1	7
BK4	7.9	6
BK5	4.6	7
BK6	6.1	7
BK7	4.8	7
LB1	4.0	6
LB2	3.8	7
LB3	4.6	6
NRM1	5.5	7
NRM2	7.7	7
SK1	4.4	7
SK2	4.4	7
SK3	5.8	7

During the production period, cell dry weight, cell morphology and pH were examined. It was found that, for all isolates and conditions, pH sharply decreased within 24 hr from initial pH at 6.5 to around pH 3 and remained along the production period. The morphological characteristics of the isolates were found to be the same. They were mostly in yeast form (blastospores) and then started to germinate at day 7 (Table 9). Isolate SK3 also produced hyphae. Typical pigment isolates (BK4 and BK6) released large amount of melanin since day 3 of cultivation. Color variant isolates remained creamy along 7 days. The profiles of cell dry weight were associated with that of EPS for all isolates.

Table 9 Morphological observation using bright-field microscope of *Aureobasidium* isolates during EPS production

Aureobasidium strain	Production period (day)	Morphotype
BK4	3	blastospores
	5	blastospores
	7	germinating blastospores
BK6	3	blastospores
	5	blastospores
	7	germinating blastospores
LB3	3	blastospores
	5	blastospores
	7	germinating blastospores
NRM2	3	blastospores
	5	blastospores
	7	germinating blastospores
SK3	3	blastospores
	5	blastospores + hyphae
	7	blastospores + hyphae

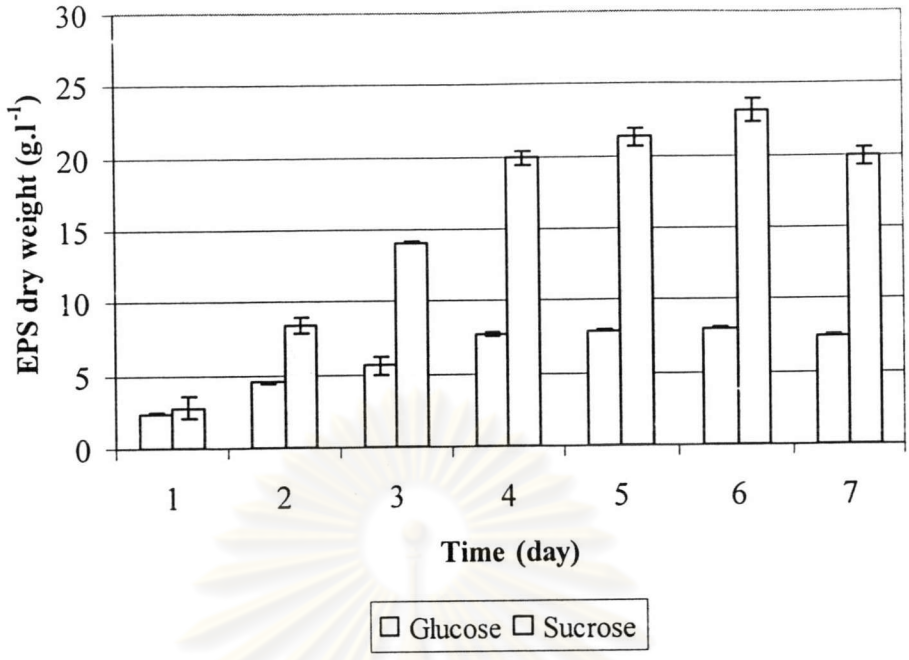

Figure 37 Effect of carbon upon EPS production by *Aureobasidium* BK4

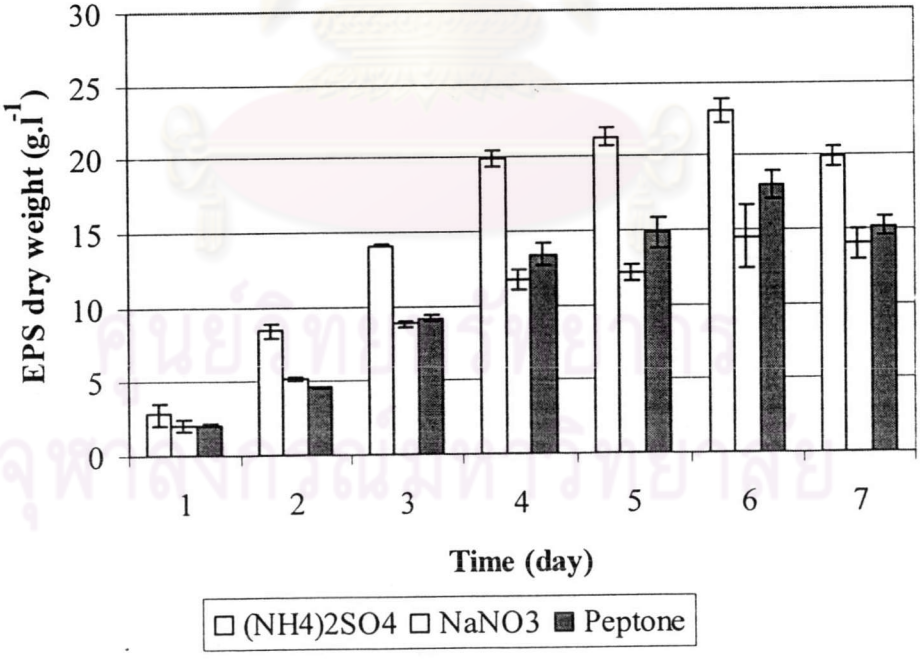

Figure 38 Effect of nitrogen upon EPS production by *Aureobasidium* BK4

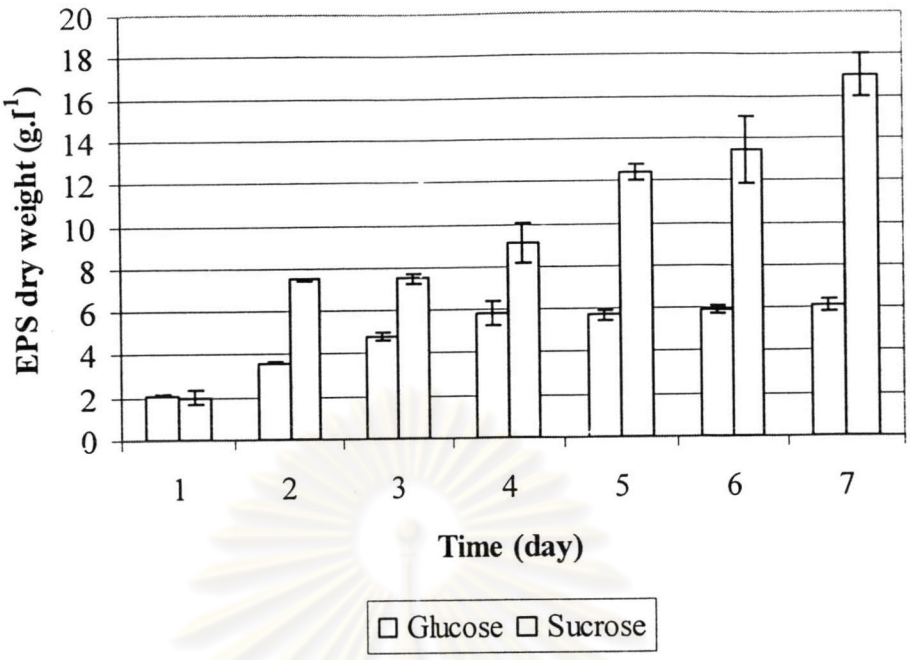

Figure 39 Effect of carbon upon EPS production by *Aureobasidium* BK6

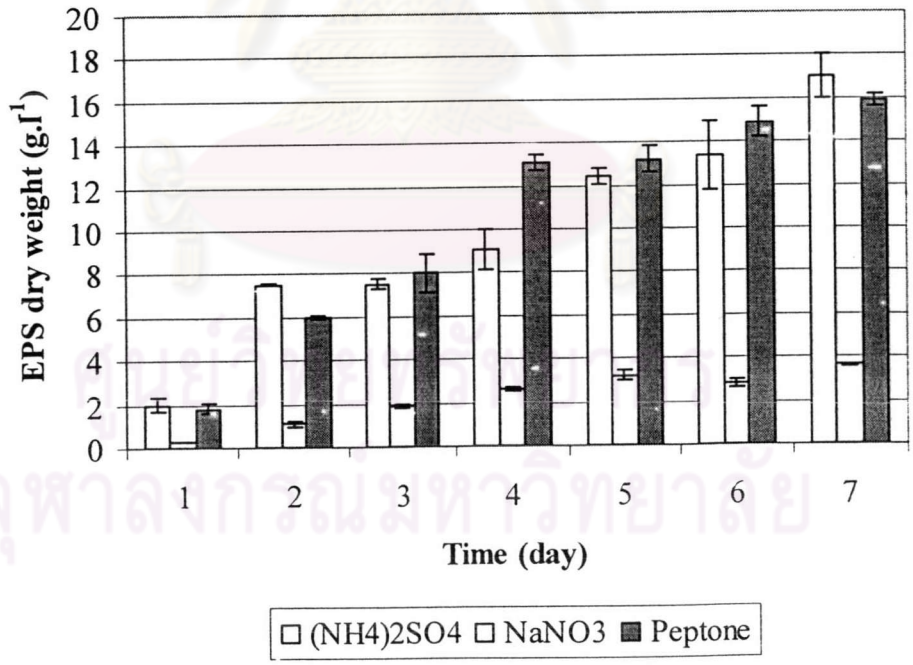

Figure 40 Effect of nitrogen upon EPS production by *Aureobasidium* BK6

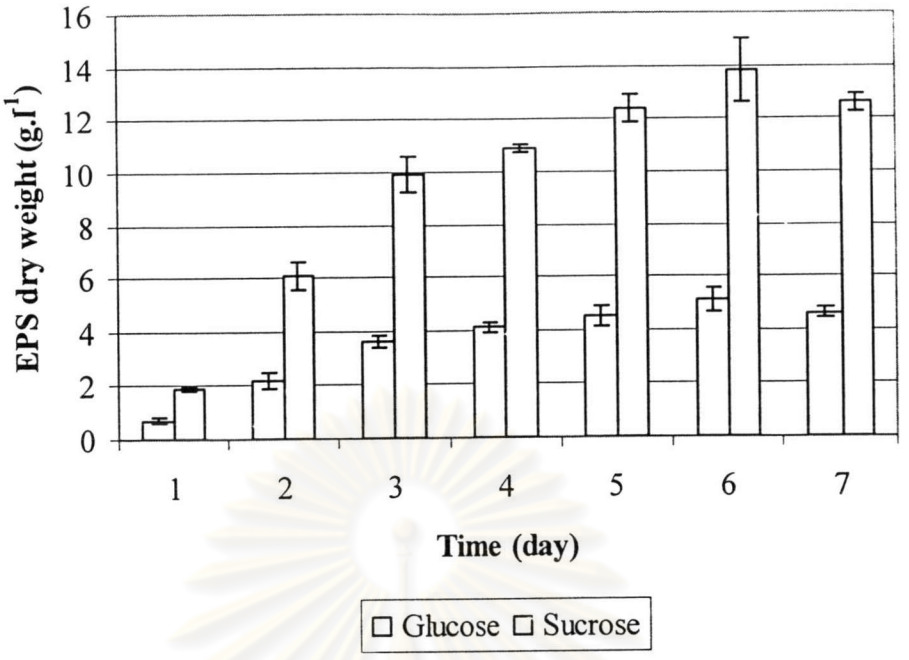

Figure 41 Effect of carbon upon EPS production by *Aureobasidium* LB3

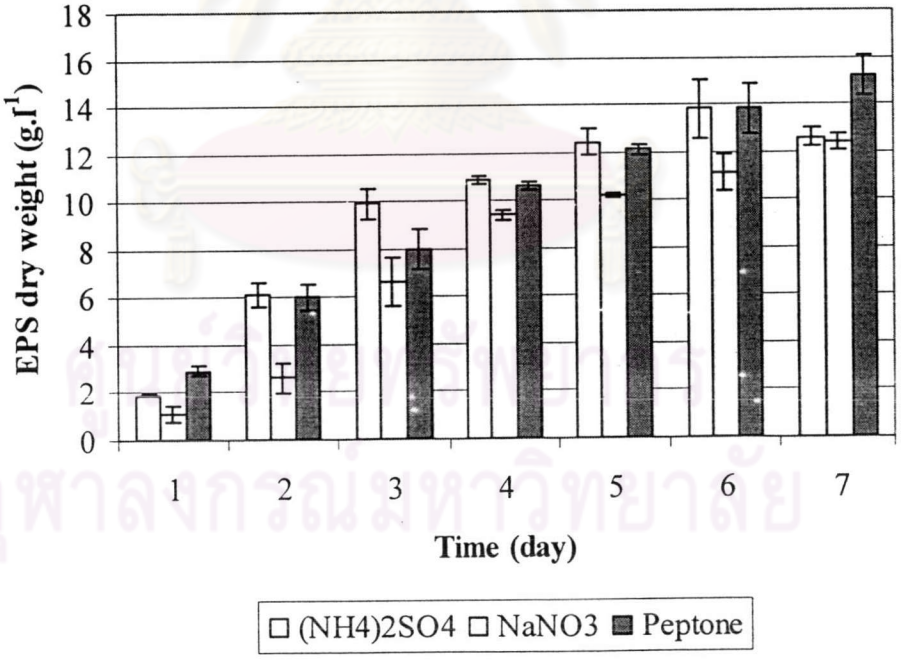

Figure 42 Effect of nitrogen upon EPS production by *Aureobasidium* LB3

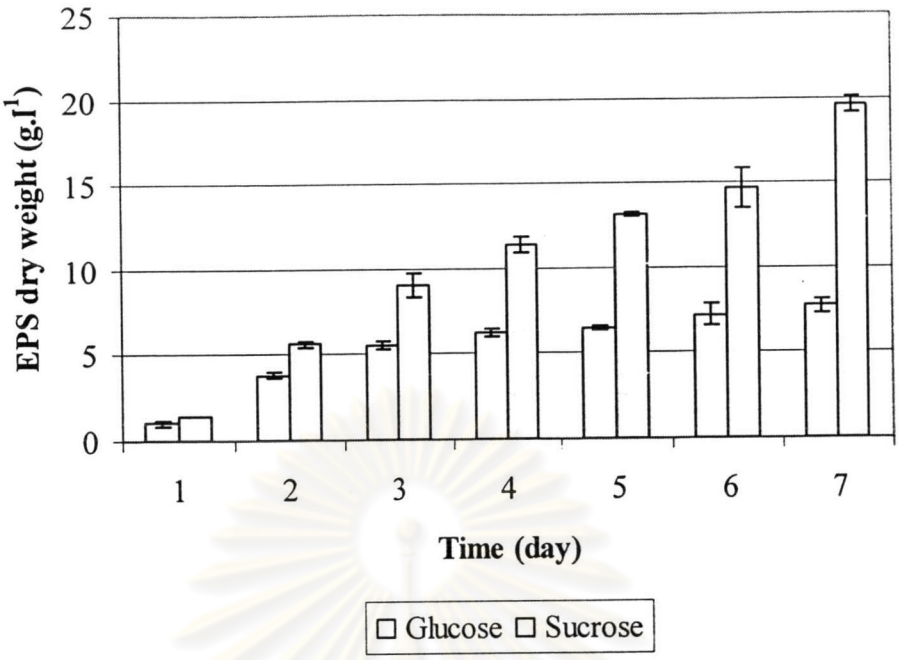

Figure 43 Effect of carbon upon EPS production by *Aureobasidium* NRM2

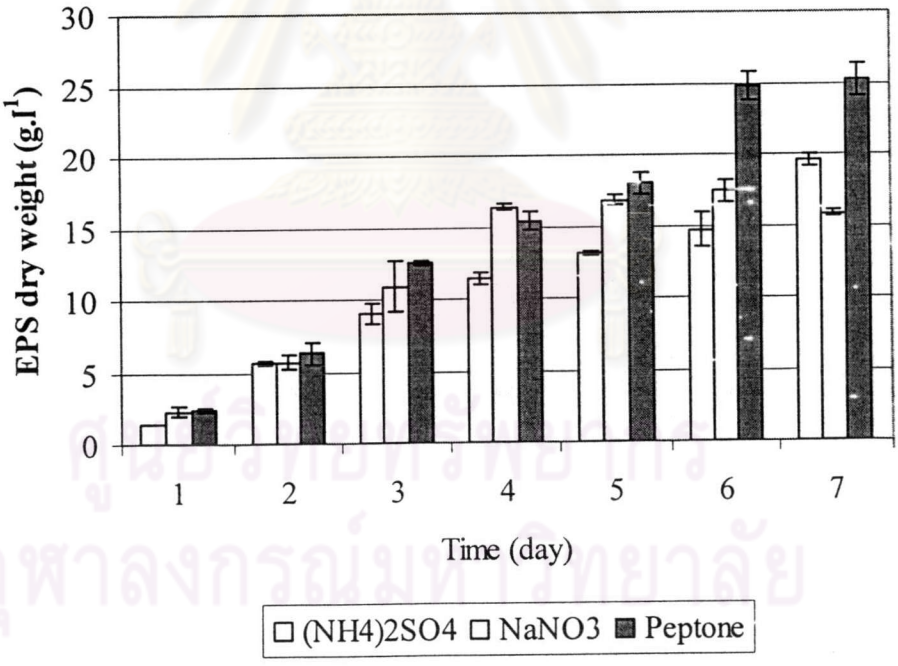

Figure 44 Effect of nitrogen upon EPS production by *Aureobasidium* NRM2

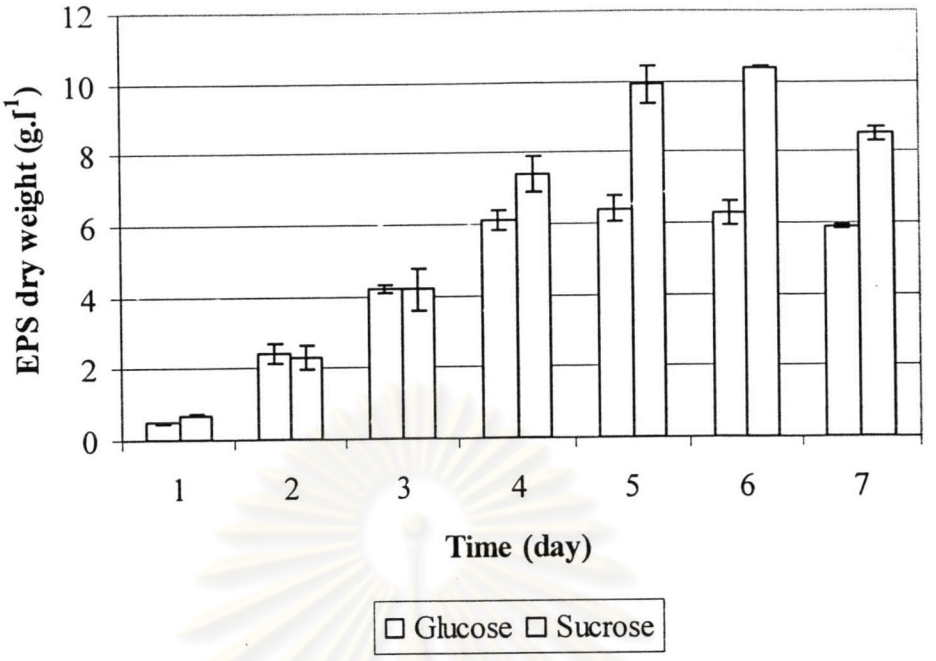

Figure 45 Effect of carbon upon EPS production by *Aureobasidium* SK3

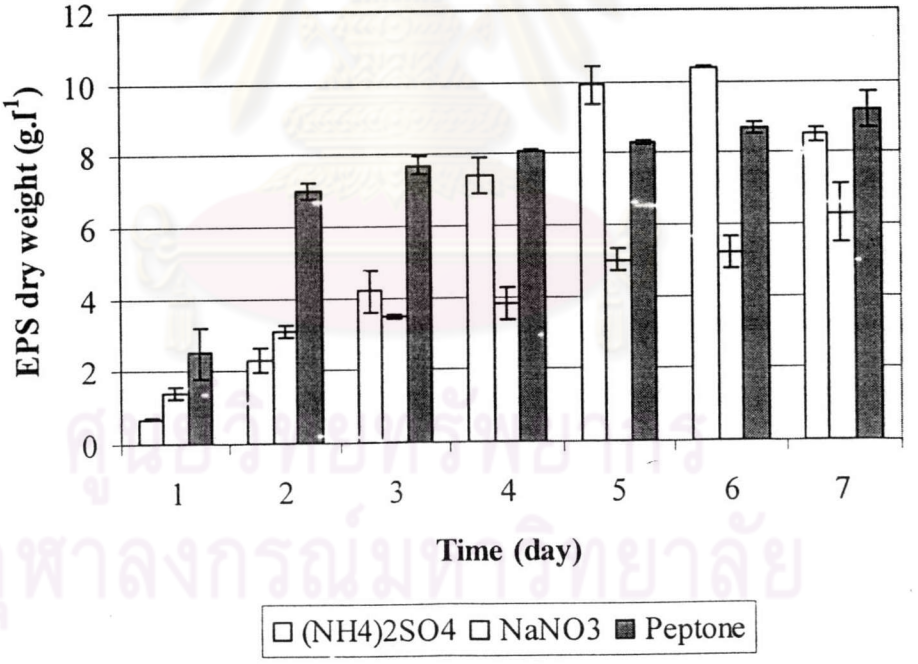

Figure 46 Effect of nitrogen upon EPS production by *Aureobasidium* SK3

4. Exopolysaccharide (EPS) analysis

4.1 Total hexose content

The EPS samples were analyzed for total hexose content by the anthrone assay, with digestion in concentrated sulfuric acid. All EPSs had a high hexose content ranging from 95-99% (Table 10). The EPS from *Aureobasidium* SK3 had the highest hexose content (99%) while the lowest ones were EPSs from *Aureobasidium* BK6 (97%) (Table 10).

4.2 Pullulanase sensitivity test

The EPS of all isolates showed sensitivities to pullulanase between 56-97% (Table 10). The EPS of *Aureobasidium* BK4 was the highest pullulanase-sensitive EPS while the EPS from *Aureobasidium* BK6 was the lowest pullulanase-sensitive EPS. Degree of pigmentation examined by visual observation showed that EPSs from *Aureobasidium* BK6 had highest pigment content (Table 10).

4.3 Infared analysis

Infared spectra (IR) of the EPSs were compared to a pullulan standard (Sigma, USA) (Figure 47). The IR analysis revealed specific functional groups (Table 11) including alkane, carbonyl, ether, hydroxyl, hydroxyl bonding in alcohol, primary alcohol, and α-configuration. Comparison of the IR spectra was presented (Table 11).

The spectra from the isolate EPSs were similar to each other and were very similar to those of the pullulan standard. The pullulan-like peak at around $\lambda = 850\ cm^{-1}$ indicates the α-configuration. Thus the IR analyses aided confirmation of the nature of the EPSs are pullulan.

Table 10 Total hexoses and pullulanase sensitivities of all EPSs.

EPS from strain	Total hexose (%)	Pullulanase sensitivities (%)	Degree of pigmentation*
BK4	98	97	+
BK6	97	56	+++
LB3	98	80	+
NRM2	97	62	++
SK3	99	90	+

*Degree of pigmentation was examined by visual observation

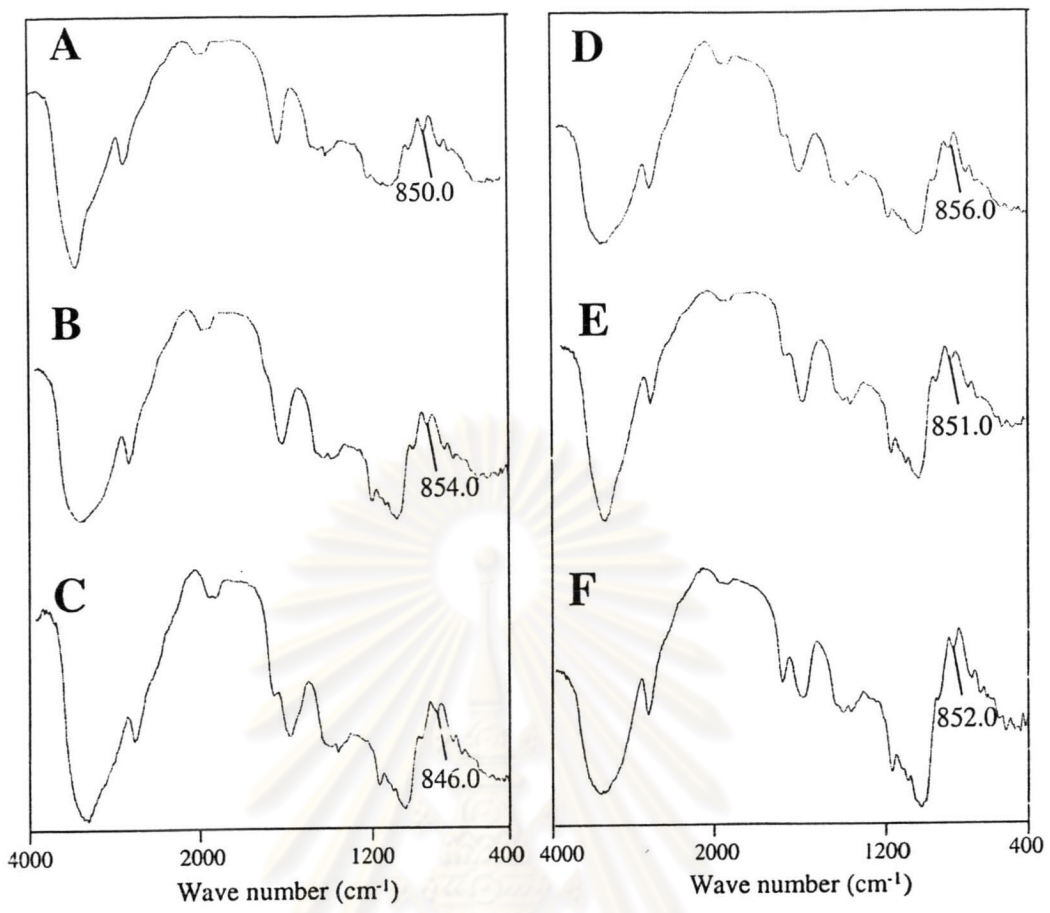

Figure 47 Infrared (IR) Spectra. (A) Pullulan (Sigma), (B) EPS from *Aureobasidium* BK4, (C) EPS from *Aureobasidium* BK6, (D) EPS from *Aureobasidium* NRM2, (E) EPS from *Aureobasidium* LB3

Table 11 Functional group of pullulan and EPS detected by IR spectra

Functional group	IR spectra (cm^{-1})					
	Pullulan (Sigma)	EPS from BK4	EPS from BK6	EPS from LB3	EPS from NRM2	EPS from SK3
-OH	3432.0	3404.0	3415.0	3469.0	3438.0	3438.0
-C-H	2931.0	2928.0	2931.0	2926.0	2929.0	2928.0
C=O	2152.0	2153.0	2075.0	2076.0	2076.0	2064.0
-C-OH	1422.0	1421.0	1423.0	1431.0	1420.0	1423.0
-OH bonding in alcohol	1384.0	1378.0	1384.0	1383.0	1384.0	1382.0
C-O	1084.0	1083.0	1083.0	1081.0	1083.0	1082.0
α-configuration	850.0	854.0	846.0	851.0	856.0	852.0

4.4 ^{13}C-NMR Spectroscopy

Structural characterization of the EPSs by ^{13}C-NMR spectroscopy yielded spectra that were typical of pullulan standard (Figures 48-53). The NMR spectra of the EPSs confirmed the homogeneity of pullulan and absence of other glucans. Three signals of anomeric carbon region were revealed at 100.8, 100.4, and 98.4 ppm. The signals at 100.8 and 100.4 corresponded to the attachment of C-1 to neighbor C-4, indicative of the two α-1,4 glucosidic linkages. Another signal at 98.4 ppm correlated to the α-1,6 glucosidic bond (C-1 attached to C-6). The results indicate a pullulan (Gorin, 1981) with a ratio of α-1,4 to α-1,6 was 2:1 (1,4:1,6) which correlated well with the structure of pullulan. The comparison of spectra is shown in Table 12.

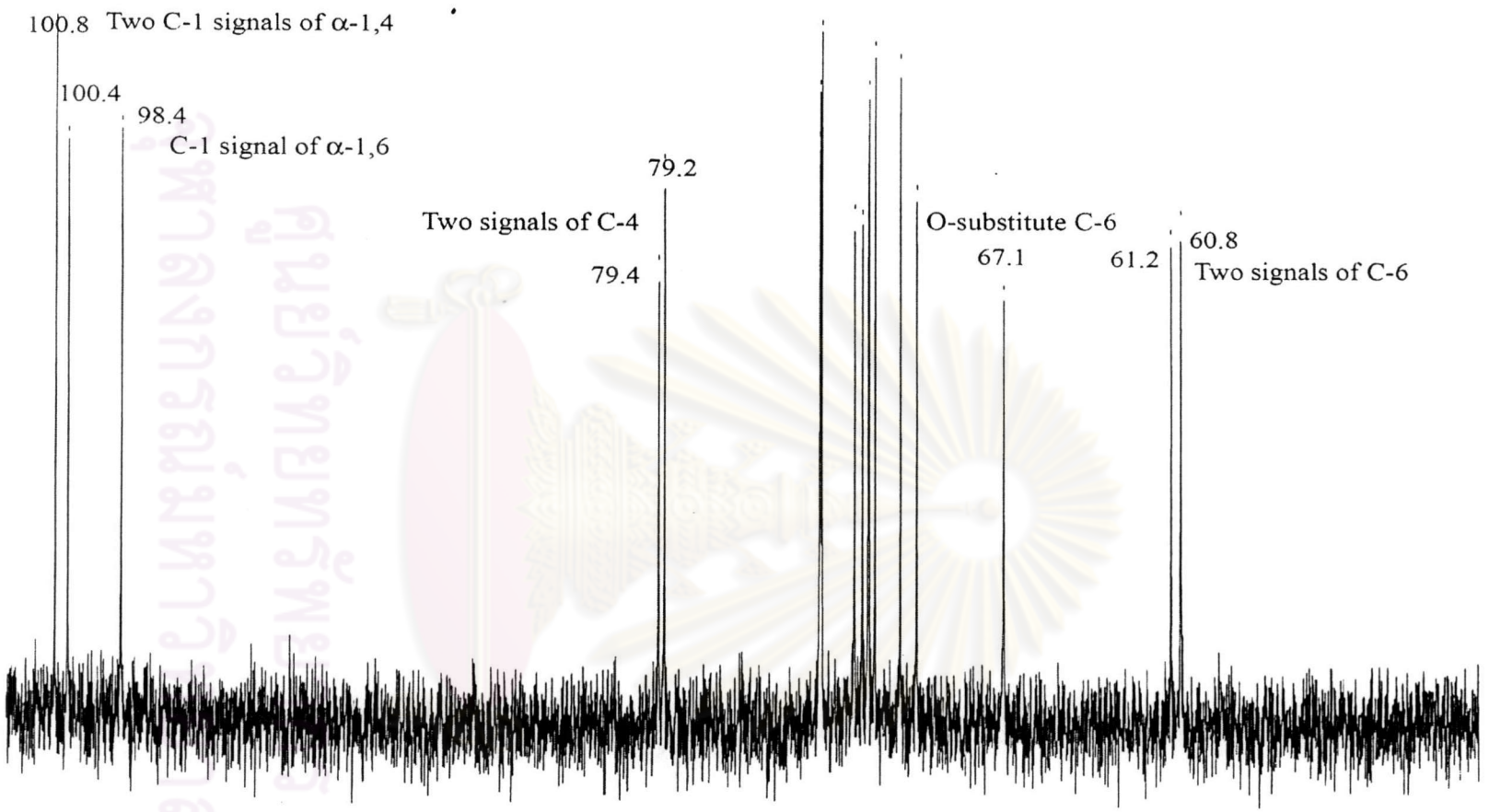

Figure 48 ^{13}C-NMR spectrum of pullulan (Showa Denko K.K., Japan)

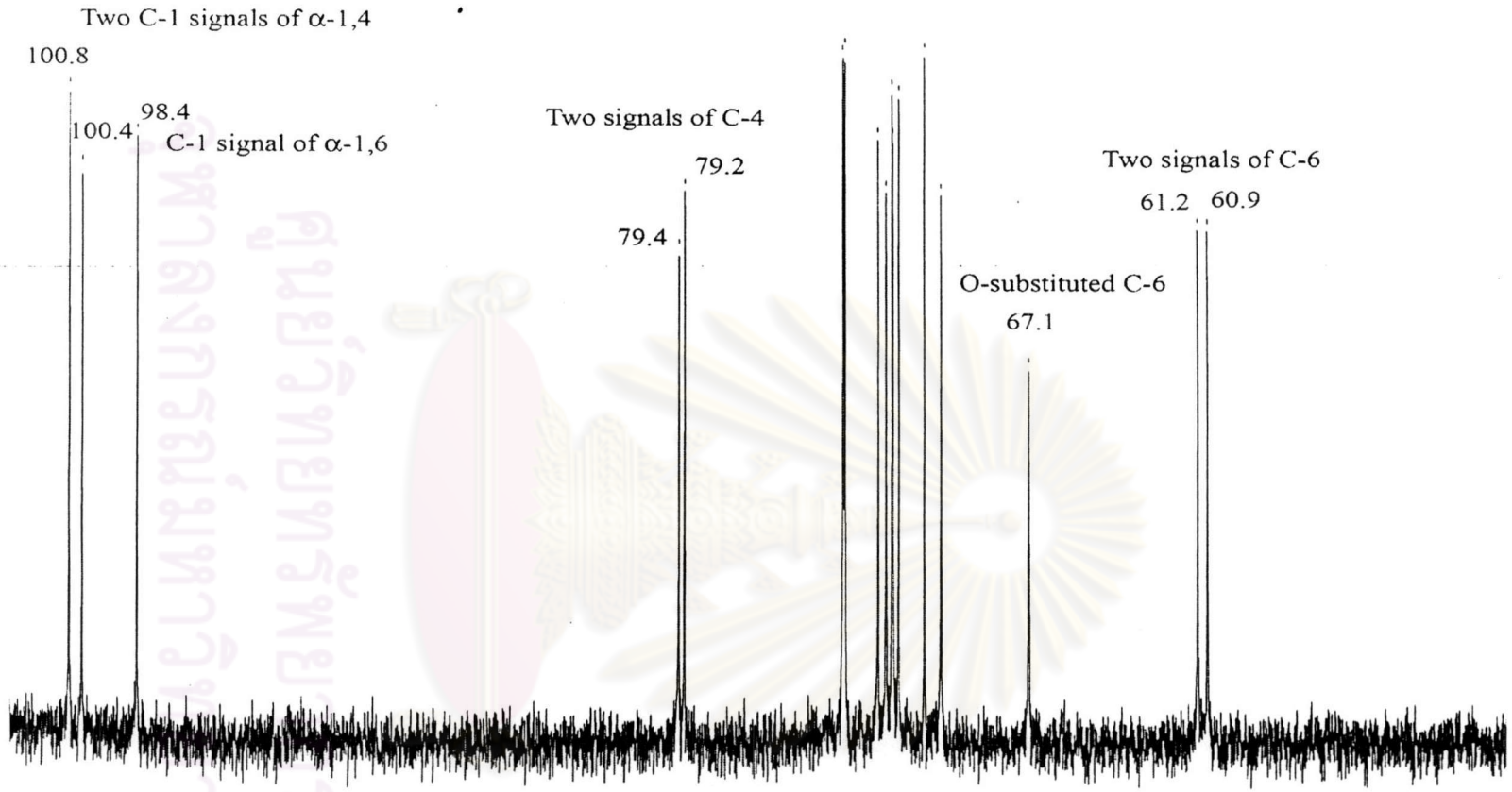

Figure 49 ^{13}C-NMR spectrum of EPS from *Aureobasidium* BK4

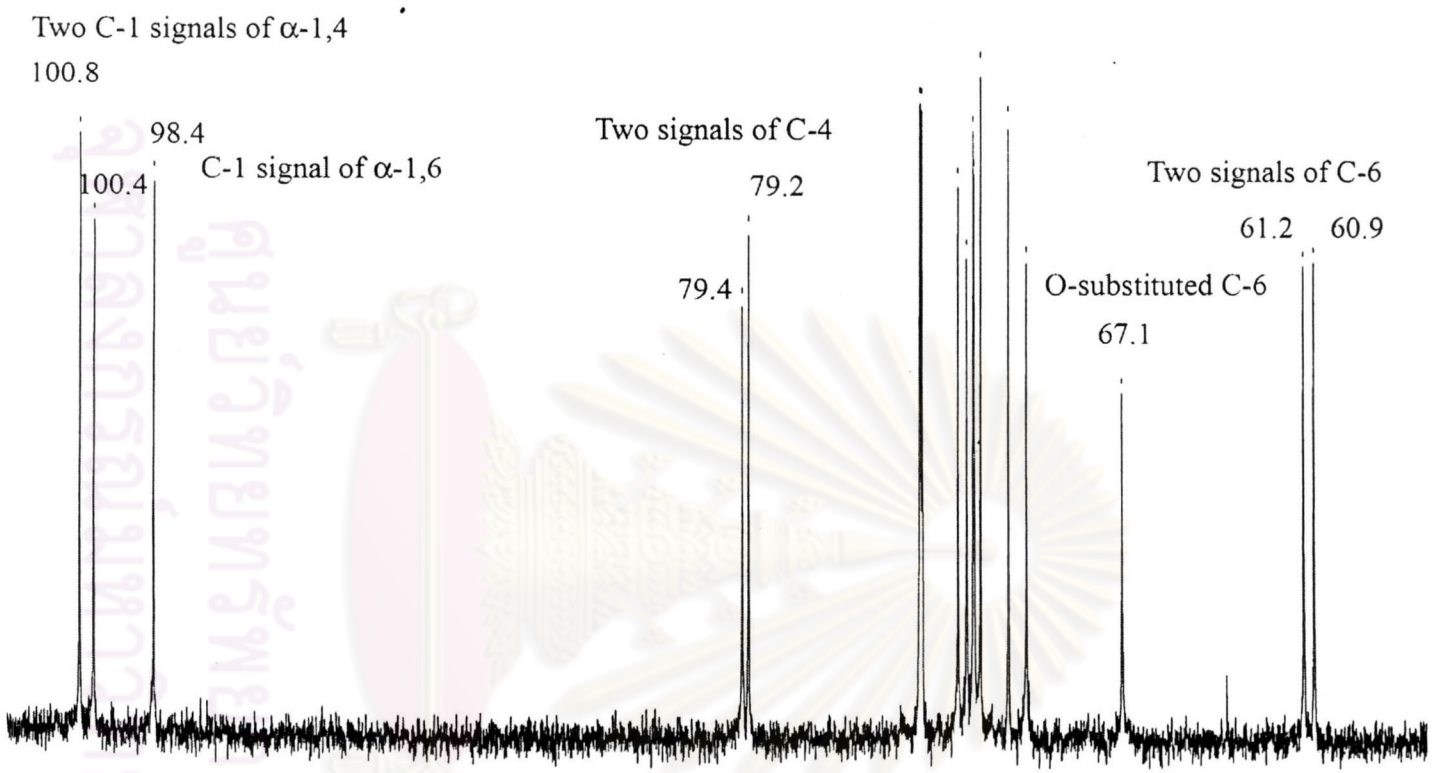

Figure 50 ^{13}C-NMR spectrum of EPS from *Aureobasidium* BK6

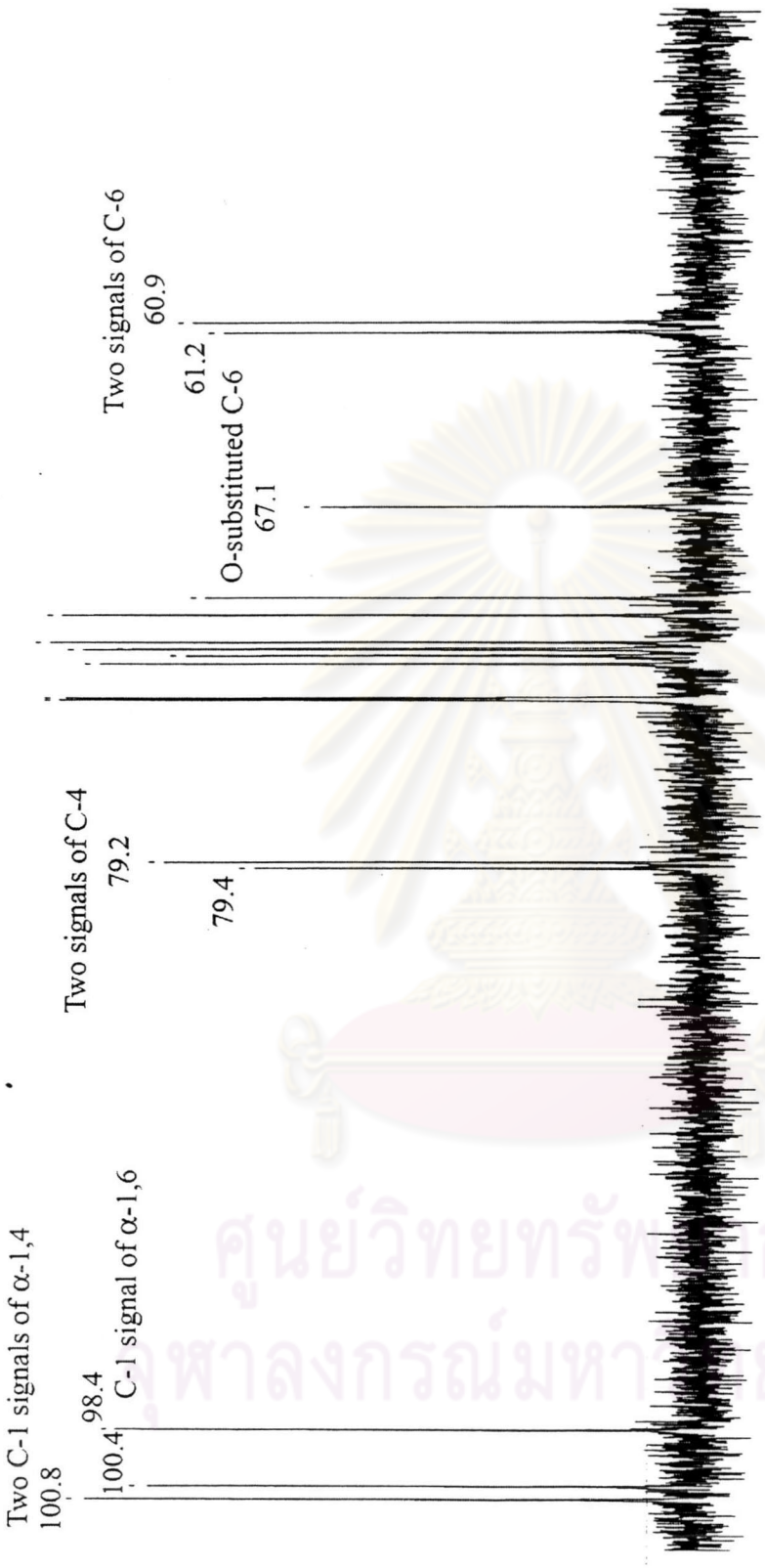

Figure 51 ^{13}C-NMR spectrum of EPS from *Aureobasidium* LB3

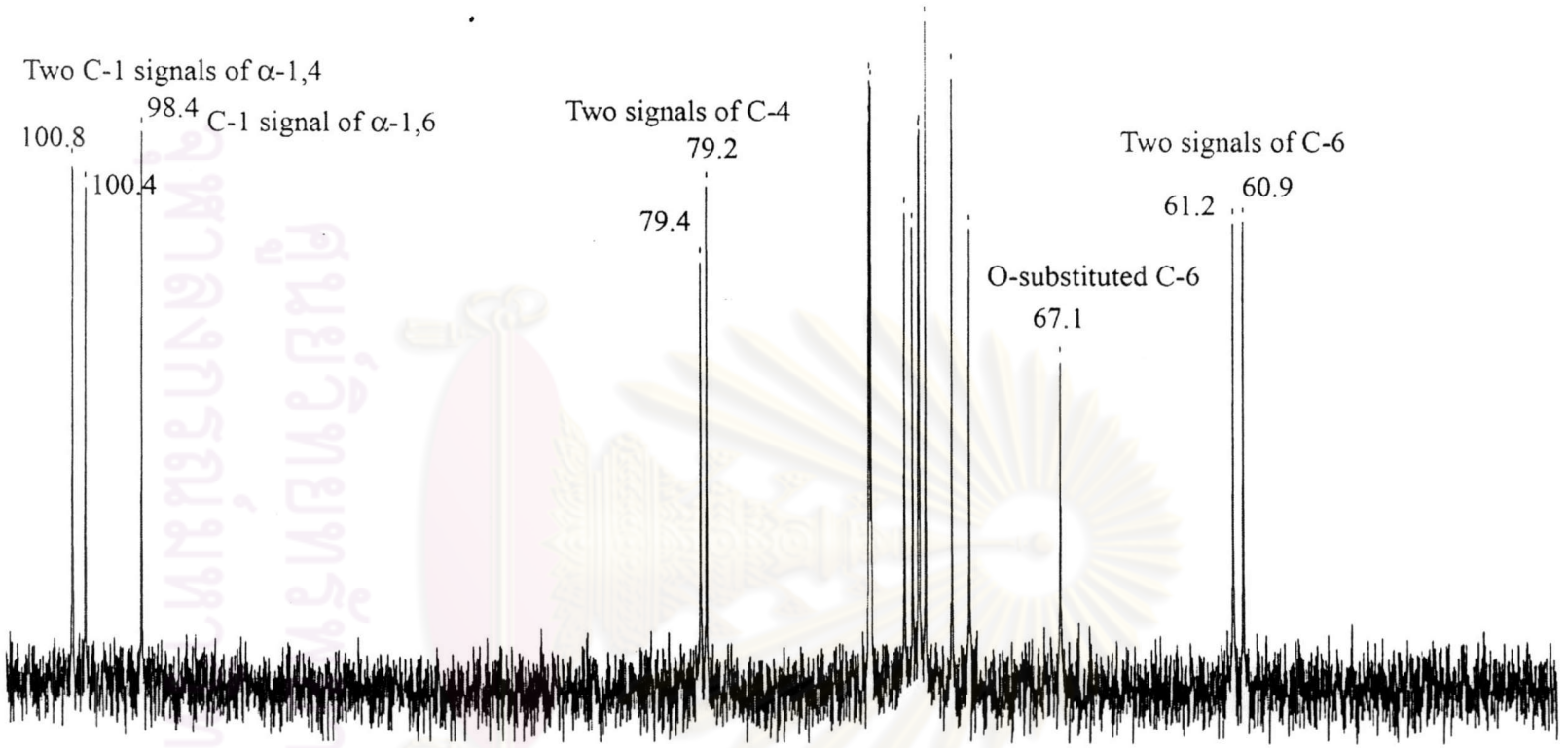

Figure 52 ^{13}C-NMR spectrum of EPS from *Aureobasidium* NRM2

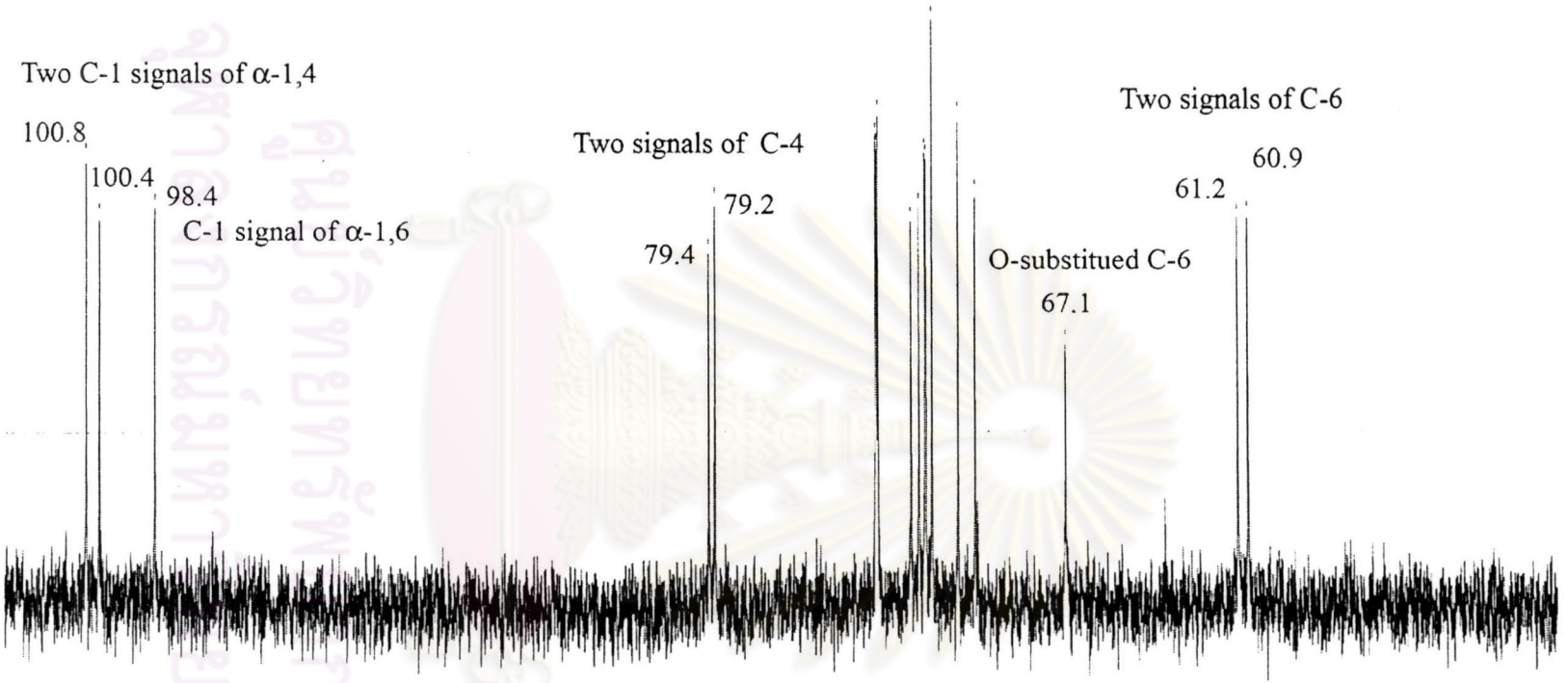

Figure 53 ^{13}C-NMR spectrum of EPS from *Aureobasidium* BK4

Table 12 Comparison of chemical shift of 13C-NMR spectra for all EPSs

Signal	13C-NMR chemical shift (ppm.)					
	Pullulan (Showa Denko K.K.)	EPS from BK4	EPS from BK6	EPS from LB3	EPS from NRM2	EPS from SK3
C-1 of α-1,4	100.8 and 100.3	100.8 and 100.3	100.8 and 100.3	100.8 and 100.3	100.8 and 100.3	100.8 and 100.3
C-1 of α-1,6	100.3	98.4	98.4	98.4	98.4	98.4
C-4	98.4 79.4 and 79.2	79.4 and 79.2	79.4 and 79.2	79.4 and 79.2	79.4 and 79.2	79.4 and 79.2
O-substituted C-6	67.1	67.1	67.1	67.1	67.1	67.1
C-6	61.2 and 60.9	61.2 and 60.9	61.2 and 60.9	61.2 and 60.9	61.2 and 60.9	61.2 and 60.9

4.5 Molecular weight and viscosity analyses

The EPSs were recovered at days 3, 5 and 7 and their molecular weights assessed using HPSEC using light scattering and refractive index for detection (see materials and methods). The molecular weights of the EPSs decreased late in culture from a range of 547,000-2,450,000 Da at day 3 to 10,200-167,000 Da by day 7 (Table 13). The highest EPS molecular weights were from isolate BK6 and NRM2 namely 2,450,000 and 1,770,000 Da on day 3. The smallest EPS was from isolate LB3 being 10,200 Da at day 7 (Table 13). For EPSs from *A. pullulans* BK4, two high-molecular weight polymers were recovered at day 3 and were both smaller by day 5. On day 7, only a single EPS was apparent. This trend was found with the EPSs from *A. pullulans* LB3 and SK3 but with only a single low-molecular weight EPS polymer present on day 5. For *A. pullulans* BK6 three large EPSs were recovered on day 3, and they were reduced to two low-molecular weight polymers and an apparent single polymer on day 5 and day 7, respectively.

For *A. pullulans* NRM2, two high-molecular weight EPS polymers and one of lower molecular weight were observed from EPS of *A. pullulans* NRM2 and they were degraded into an apparent single low-molecular weight polymer by day 5 and day 7 (Table 13). The trend from high molecular weight EPS to a smaller size was universal with the cultures tested.

4.5.2 Viscosity of EPS

The viscosities of the EPS were recorded using a Brookfield viscometer. The viscosities of the EPSs were compared to the molecular weight data (Tables 13 and 14). The viscosities decreased from 17.41-3.49 cP on day 3 to 2.63-1.53 cP on day 7. The highest viscosity EPS was from isolate BK6 (17.41 cP) on day 3 and the lowest viscosity EPS was from isolate SK3 on day 7 (Table 14).

The decrease of EPS molecular weights and viscosities in late culture might be the result from extracellular alpha-amylase or pullulanase enzymes. It was decided that such enzymes should be assessed from all strains.

5. Enzyme assays

5.1 Alpha amylase screening

Aureobasidium cultures were screened for alpha-amylase activity using a starch agar plate assay. After the culture for 5 days the plates were flooded with iodine solution and the presence of any clear haloes around the colonies assessed. All *Aureobasidium* cultures were positive (Figure 54). Strain SK3 grew very slowly on the starch agar plate, yet also formed a clear halo. It was clear that all *Aureobasidium* strains produced alpha-amylase when cultured on starch.

5.2 Alpha-amylase and pullulanase activities assay

The culture supernatant from the starch (1%) and sucrose (1%) cultures at day 5 and day 7 were assayed for alpha-amylase and pullulanase activities. Substrates were borohydride-reduced starch and borohydride-reduced pullulan respectively. All cultures exhibited alpha-amylase activity higher than pullulanase activity (Tables 15 and 16). The maximal alpha-amylase activity was from *Aureobasidium* NRM2 grown on starch on day 7 (0.738 $U.ml^{-1}$) while the maximum pullulanase activity was produced by strain BK6 at 5 days (0.040 $U.ml^{-1}$). The lowest alpha-amylase and pullulanase yields were from *Aureobasidium* SK3 on day 7. On sucrose (1%) medium, *A. pullulans* also produced alpha-amylase, ranging from 0.024 up to 0.408 $U.ml^{-1}$, and pullulanase ranging from 0.002 to 0.013 $U.ml^{-1}$ dependent on the culture (Table 10). The highest alpha-amylase yield from sucrose grown cells was from *A. pullulans* NRM2 on day 7 (0.408 $U.ml^{-1}$) while the highest pullulanase activity was

from *Aureobasidium* BK4 (0.013 $U.ml^{-1}$) (Tables 15 and 16). Clearly all *Aureobasidium* strains tested produced alpha-amylase and pullulanase when grown either on starch or sucrose.

Table 13 Molecular weight of EPSs from *A. pullulans* at day 3, 5, 7 of production period

EPSs from *Aureobasidium* strain	Production period (day)	Number of polymer	Molecular weight (Da)
BK4	3	2	580,000/ 335,000
	5	2	151,000/ 86,700
	7	1	13,300
BK6	3	3	2,450,000/ 562,000/ 27,000
	5	2	372,000/19,400
	7	1	22,400
LB3	3	2	385,000/ 162,000
	5	1	27,500
	7	1	10,200
NRM2	3	3	1,770,000/ 1,320,000/ 30,500
	5	1	315,000
	7	1	167,000
SK3	3	2	470,000/ 113,000
	5	1	149,000
	7	1	147,000

Table 14 Viscosity of EPSs from *Aureobasidium* spp. at day 3, 5, 7 of production period

EPSs from *Aureobasidium* strain	Production period (day)	Viscosity (cP)
BK4	3	15.26
	5	4.50
	7	2.50
BK6	3	17.41
	5	2.84
	7	2.15
LB3	3	6.05
	5	2.63
	7	2.60
NRM2	3	15.25
	5	3.18
	7	2.15
SK3	3	3.49
	5	2.56
	7	1.53

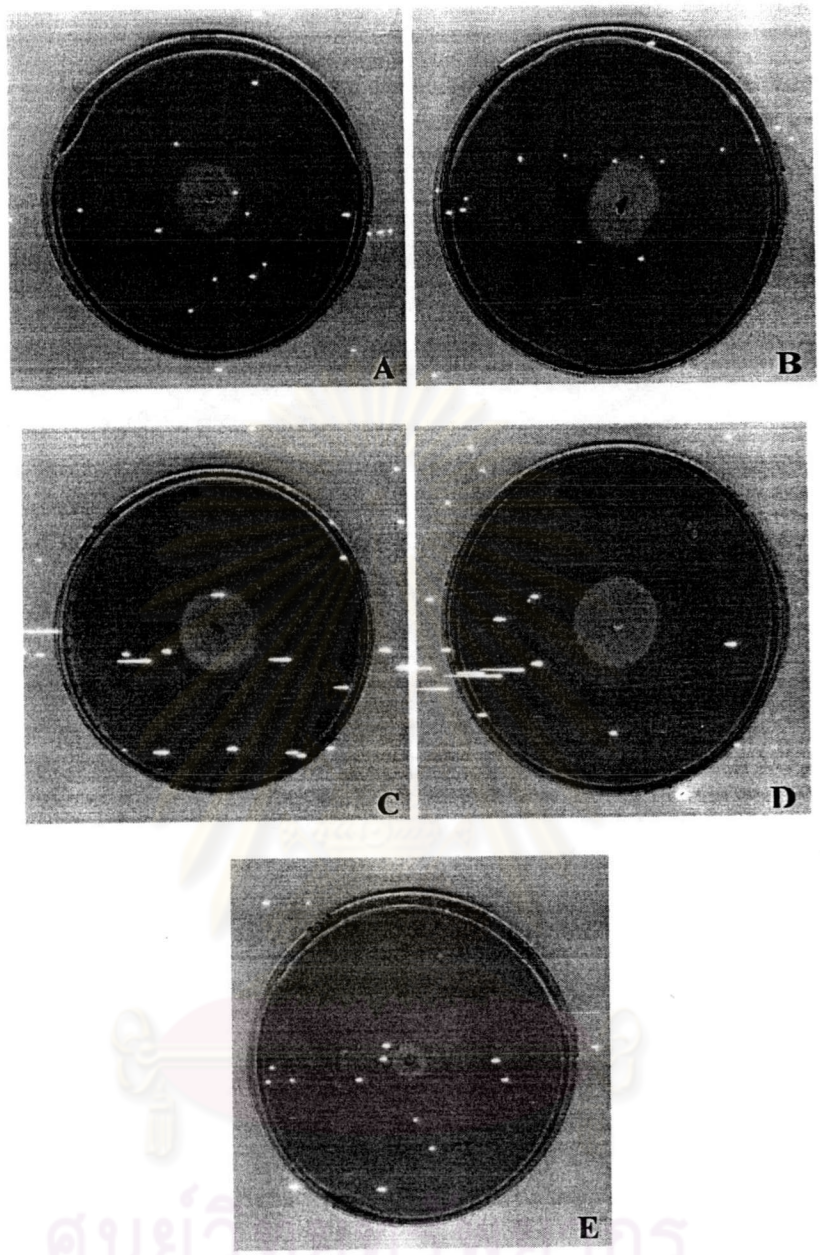

Figure 54 Alpha-amylase/iodine screening of *Aureobasidium* strains. (A) *Aureobasidium* BK4, (B) *Aureobasidium* BK6, (C) *Aureobasidium* LB3, (D) *Aureobasidium* NRM2, (E) *Aureobasidium* SK3

Table 15 Alpha-amylase and pullulanase activities of culture supernatant of *Aureobasidium* grown on starch (1%) medium

A. pullulans	Alpha-amylase (U/ml)		Pullulanase (U/ml)	
	Day 5	Day 7	Day 5	Day 7
BK4	0.250	0.402	0.036	0.020
BK6	0.153	0.230	0.040	0.024
LB3	0.247	0.176	0.029	0.010
NRM2	0.695	0.738	0.016	0.017
SK3	0.135	0.130	0.033	0.009

Table 16 Alpha-amylase and pullulanase activities of culture supernatant of *Aureobasidium* grown on sucrose (1%) medium

A. pullulans	Alpha-amylase (U/ml)		Pullulanase (U/ml)	
	Day 5	Day 7	Day 5	Day 7
BK4	0.070	0.186	0.007	0.013
BK6	0.053	0.129	0.005	0.009
LB3	0.065	0.134	0.004	0.002
NRM2	0.170	0.408	0.004	0.005
SK3	0.024	0.100	0.004	0.004

5.3 Alpha-amylase zymogram of native electrophoresis gel

Crude culture supernatants of the *Aureobasidium* cultures grown on starch (1%) and sucrose (1%) were subjected to native electrophoresis gel and assessed for the presence of alpha-amylase activity via iodine staining. The electrophoresis gel was soaked in 2% starch solution (in 50 mM acetate buffer pH 5.0) for 3 hr at 50°C. Alpha-amylase activity was detected by staining the starch based gel with iodine.

The culture supernatants of all *Aureobasidium* strains grown on both substrates produced amylases (Figure 55). When grown on starch, *Aureobasidium* BK4, BK6 and NRM2 produced two bands of alpha-amylase activity while strains *Aureobasidium* LB3 and SK3 only produced a single band. Furthermore only a single activity band was produced when all cultures were grown on sucrose. The amylases were in extremely very low concentration in that staining with Comassie Blue failed to detect protein at an equivalent position to the amylase activity bands. However they were of high specific activity in order to have been detected.

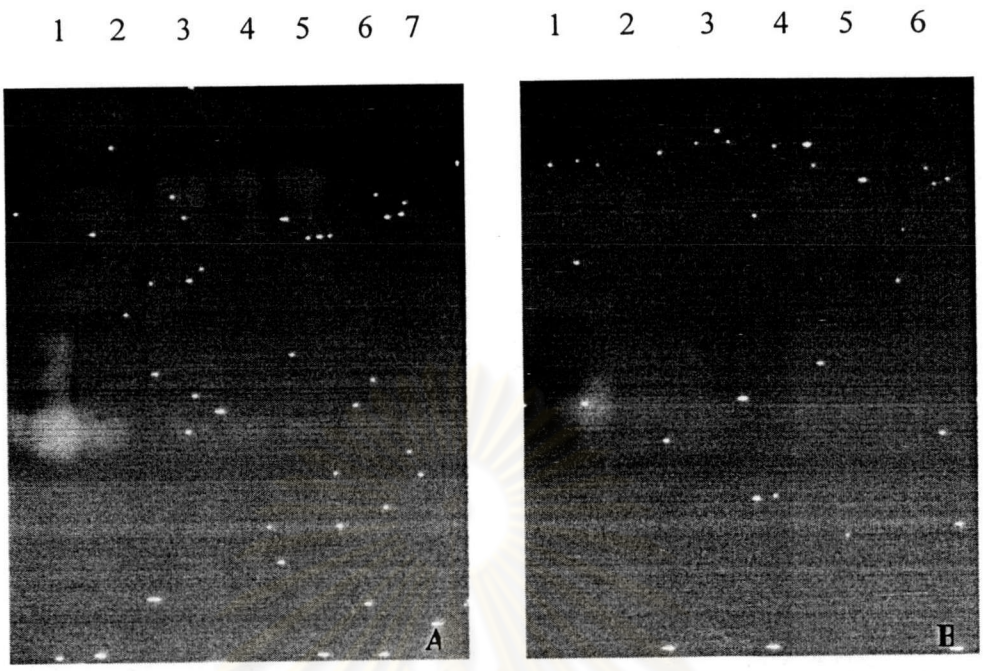

Figure 55 Native electrophoresis gels of alpha-amylase activities of culture supernatant of *Aureobasidium* strains grown on starch and sucrose medium. (A) Culture supernatants from starch (1%) medium, (B) Culture supernatants from sucrose (1%) medium

Figure 55 (A)

Lane 1: alpha-amylase (Sigma)

Lane 2: negative control (culture medium)

Lane 3: *Aureobasidium* BK4

Lane 4: *Aureobasidium* BK6

Lane 5: *Aureobasidium* NRM2

Lane 6: *Aureobasidium* LB3

Lane 7: *Aureobasidium* SK3

Figure 55 (B)

Lane 1: alpha-amylase (Sigma)

Lane 2: *Aureobasidium* BK4

Lane 3: *Aureobasidium* BK6

Lane 4: *Aureobasidium* NRM2

Lane 5: *Aureobasidium* LB3

Lane 6: *Aureobasidium* SK3

6. Enhancement of the molecular weight of EPS

From the above results, *Aureobasidium* NRM2 produced high yields of pullulan (25.1 $g.l^{-1}$) by day 7. However this pullulan can be of reduced molecular weight detected by HPSEC analysis and viscosity measurement (See Tables 13 and 14). The smaller molecular weights could be a result of alpha-amylase attacking the pullulan in the late stages of the culture. Thus in order to attempt to obtain high-yield and high-quality pullulan, amylase negative mutants were prepared. The use of an amylase inhibitor present in the culture medium for pullulan production was another approach considered in this thesis.

6.1 Preparation of amylase-negative mutants using a chemical mutagen N-methyl-N'-nitro-N-nitrosoguanidine (NTG)

A high-yielding strain of *Aureobasidium* NRM2 was subjected to NTG mutagenesis. A range of concentrations (50, 100, 200, 400 μg/ml) of NTG was used, and cells were incubated with NTG (in 0.1 M phosphate buffer pH 7.0) at 28°C for 30 min. The kill curve showed a 97% kill at an NTG level of 400 μg/ml (Figure 56). Using a 97% kill 1,327 NTG treated cells yielded one amylase negative mutant, *Aureobasidium* ANM1 (Figures 57 and 58). Strain ANM1 was subcultured for five generations and then retested for alpha-amylase activity on a starch agar plate and in liquid medium (1% starch). This strain did not grow on starch either liquid or solid media. The EPS was produced from this strain, and its molecular weight was assessed using HPSEC (see materials and methods).

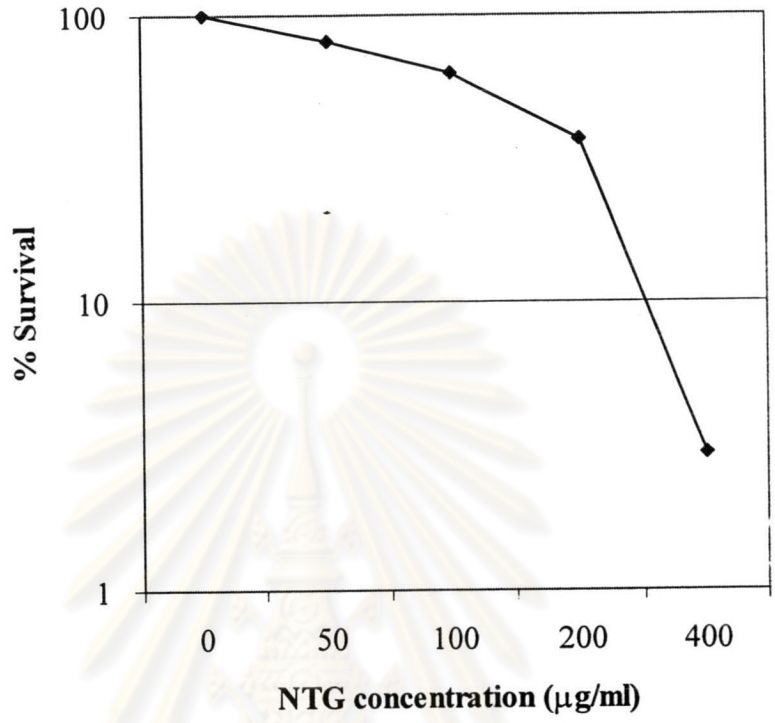

Figure 56 Survival curve of *Aureobasidium* NRM2 treated with a range of concentrations of NTG (in 0.1 M phosphate buffer pH 7.0) incubated at 28°C for 30 min

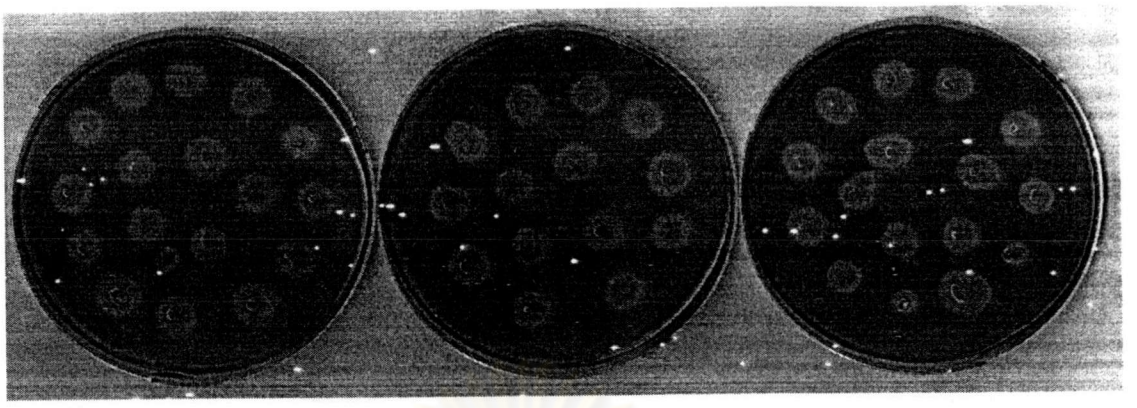

Figure 57 Alpha-amylase plates screening of amylase negative *Aureobasidium* strain NRM2.

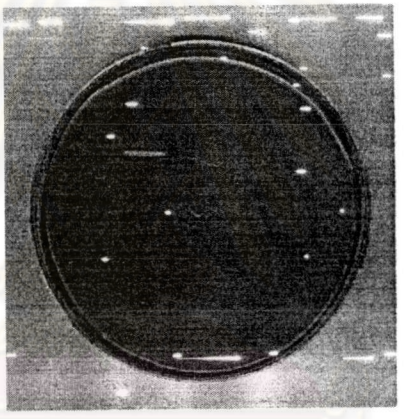

Figure 58 Alpha-amylase plate screening of *Aureobasidium* ANM1 (amylase negative via NTG mutation) with no growth or alpha-amylase production

6.2 Inhibition of amylase activity by incorporation of an amylase inhibitor (acarbose) into the EPS fermentation medium

Aureobasidium NRM2 was cultured in the presence of acarbose (50 mg/ml) in sucrose based medium. EPSs were recovered at days 3, 5, and 7 and were subjected to molecular weight analysis using HPSEC.

These molecular weights of the EPSs from the wild type strain in the presence of acarbose compared to the control lacking of acarbose are illustrated (Figures 48 and 50) (see under 6.3).

6.3 Molecular weight analysis using HPSEC for EPSs from an amylase negative mutant (ANM1) and EPSs from strain NRM2 in the presence of acarbose

All EPSs tested, including control EPSs from the wild type strain NRM2 without acarbose, EPSs from an amylase negative mutant strain (ANM1), and EPSs from strain NRM2 cultured in the presence of acarbose, showed similar molecular weight profiles (Figures 59, 60 and 61). The molecular weight of EPSs on day 3 showed major elution peaks at 10.2 min estimated as 20,000,000 Da. The considerable degradation of these initial high molecular weight EPSs on day 3 into multiple smaller polymers at day 5 and day 7 was observed with the major peaks of EPSs eluted at around 18.0 min estimated as 25,000 Da. However, the major elution peaks of EPSs from strain NMR2 in the presence of acarbose on day 5 and day 7 were found at 17.6 min estimated as 30,000 Da (Figure 50) indicated that the degradation of the EPSs from strain NRM2 in the presence of acarbose (30,000 Da) was less severe than those from strain NRM2 without acarbose (25,000 Da).

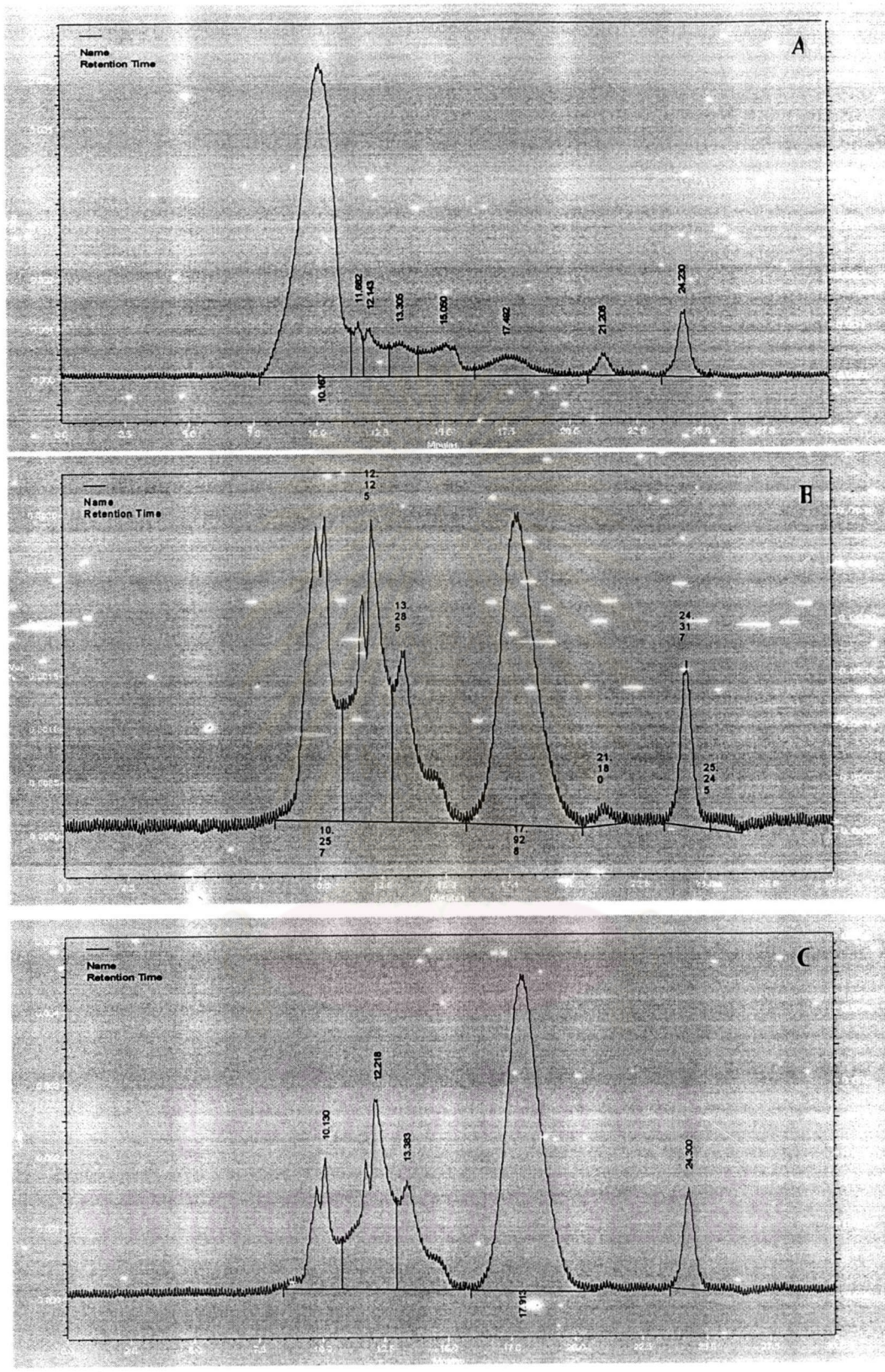

Figure 59 Molecular weight profiles of EPSs from *A. pullulans* NRM2 (without amylase inhibitor). (A) EPS on day 3, (B) EPS on day 5, (C) EPS on day 7

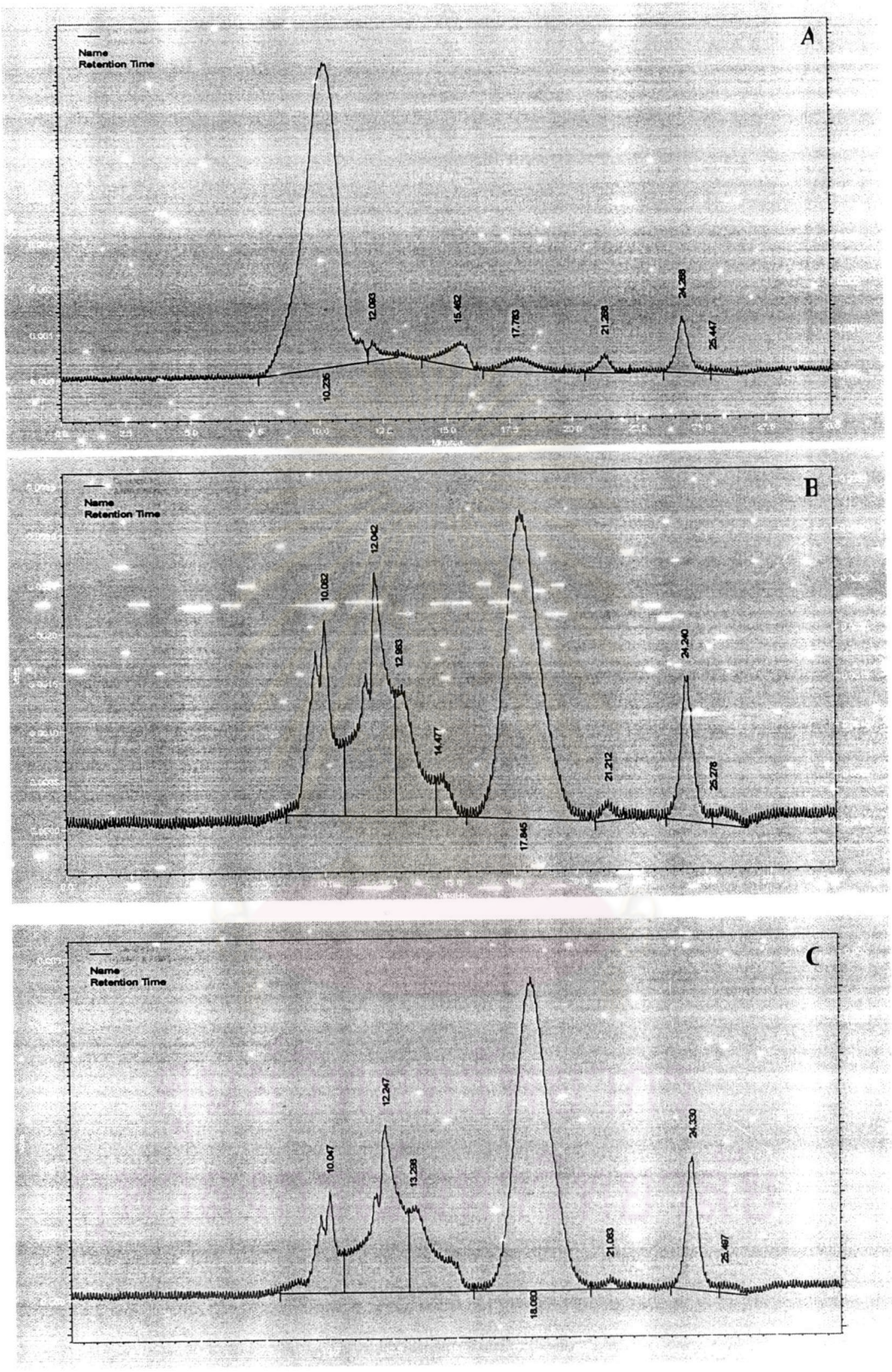

Figure 60 Molecular weight profiles of EPSs from an amylase negative mutant ANM1. (A) EPS on day 3, (B) EPS on day 5, (C) EPS on day 7

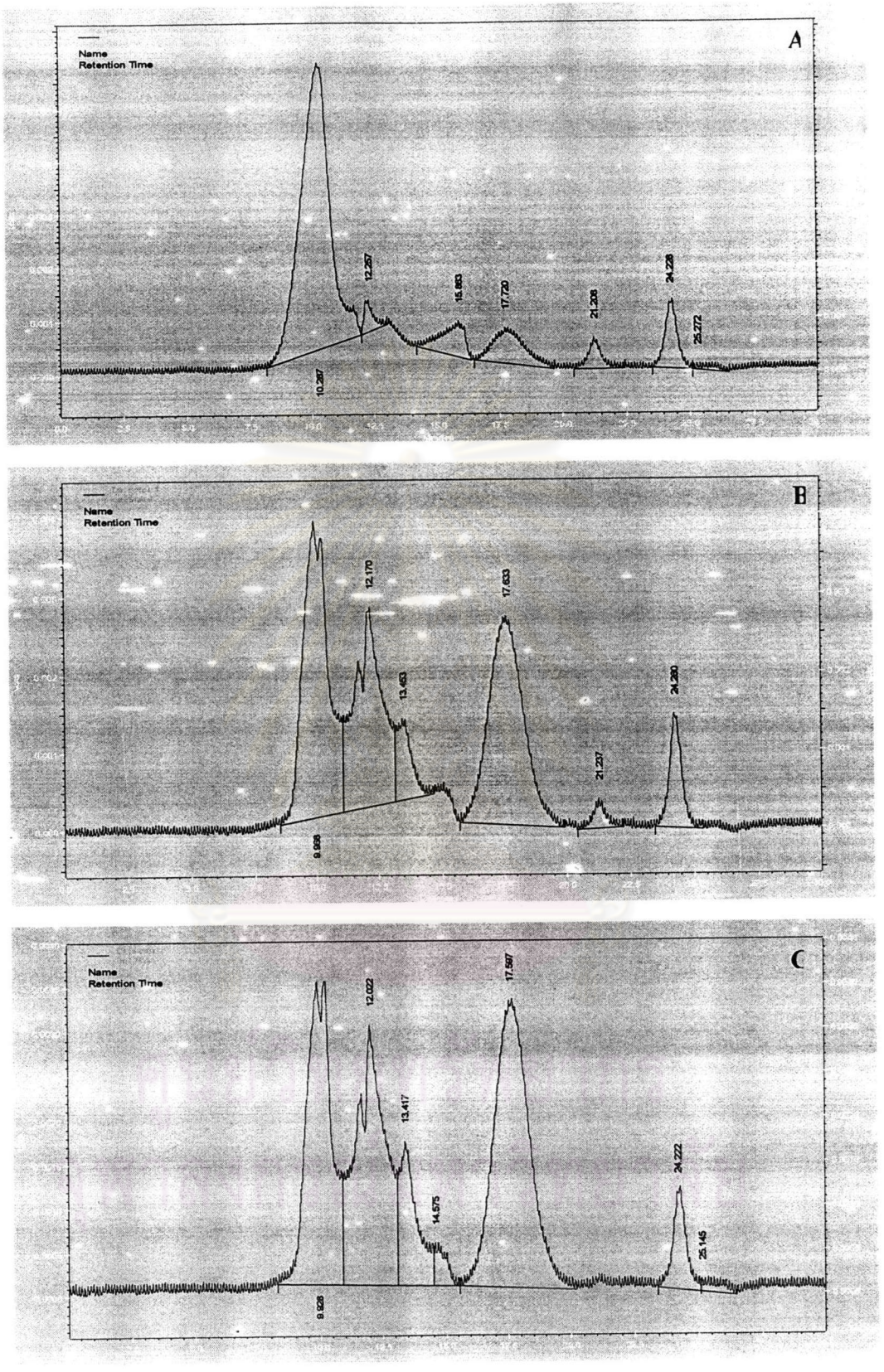

Figure 61 Molecular weight profiles of EPSs from strain NRM2 in the presence of acarbose. (A) EPS on day 3, (B) EPS on day 5, (C) EPS on day 7